



Review

Recent progress on the recycling technology of Li-ion batteries

Yuqing Wang ^{a,1}, Ning An ^{a,1}, Lei Wen ^b, Lei Wang ^a, Xiaotong Jiang ^c, Feng Hou ^{a,*}, Yuxin Yin ^d, Ji Liang ^{a,e,*}^a Key Laboratory of Advanced Ceramics and Machining Technology of Ministry of Education, School of Materials Science and Engineering, Tianjin University, Tianjin 300072, China^b Shenyang National Laboratory for Materials Science, Institute of Metal Research, Chinese Academy of Sciences, Shenyang 110016, Liaoning, China^c China Automotive Technology & Research Center Co., Ltd, Tianjin 300300, China^d Tianjin Lishen Battery Joint-Stock Limited Company, Tianjin 300384, China^e Institute for Superconducting & Electronic Materials, Australian Institute of Innovative Materials, University of Wollongong, Innovation Campus, North Wollongong, NSW 2500, Australia

ARTICLE INFO

Article history:

Received 8 March 2020

Revised 30 April 2020

Accepted 7 May 2020

Available online 19 May 2020

Keywords:

Li ion battery

Recycling

Cathode

Anode

ABSTRACT

Lithium-ion batteries (LIBs) have been widely applied in portable electronic devices and electric vehicles. With the booming of the respective markets, a huge quantity of spent LIBs that typically use either LiFePO_4 or $\text{LiNi}_{x}\text{Co}_{y}\text{Mn}_{z}\text{O}_2$ cathode materials will be produced in the very near future, imposing significant pressure for the development of suitable disposal/recycling technologies, in terms of both environmental protection and resource reclaiming. In this review, we firstly do a comprehensive summary of the-state-of-art technologies to recycle $\text{LiNi}_{x}\text{Co}_{y}\text{Mn}_{z}\text{O}_2$ and LiFePO_4 -based LIBs, in the aspects of pretreatment, hydrometallurgical recycling, and direct regeneration of the cathode materials. This closed-loop strategy for cycling cathode materials has been regarded as an ideal approach considering its economic benefit and environmental friendliness. Afterward, as for the exhausted anode materials, we focus on the utilization of exhausted anode materials to obtain other functional materials, such as graphene. Finally, the existing challenges in recycling the LiFePO_4 and $\text{LiNi}_{x}\text{Co}_{y}\text{Mn}_{z}\text{O}_2$ cathodes and graphite anodes for industrial-scale application are discussed in detail; and the possible strategies for these issues are proposed. We expect this review can provide a roadmap towards better technologies for recycling LIBs, shed light on the future development of novel battery recycling technologies to promote the environmental benignity and economic viability of the battery industry and pave way for the large-scale application of LIBs in industrial fields in the near future.

© 2020 Science Press and Dalian Institute of Chemical Physics, Chinese Academy of Sciences. Published by ELSEVIER B.V. and Science Press. All rights reserved.

Contents

1. Introduction	393
2. Recycling of the cathode materials	395
2.1. Pretreatment of exhausted LIBs	395
2.2. Hydrometallurgical regeneration of the cathode materials	396
2.2.1. Leaching and separation of metal ions	396
2.2.2. Mechanochemical-assisted metal leaching	405
2.2.3. Regeneration of cathode from the leachate	405
2.3. Direct regeneration of cathode materials	409
3. Recycling of graphite anodes	412
3.1. Regenerating graphite and recycling lithium	413
3.2. Synthesis of graphene from spent anode graphite	413
4. Discussion	415
5. Conclusions and perspective	416

* Corresponding authors at: Key Laboratory of Advanced Ceramics and Machining Technology of Ministry of Education, School of Materials Science and Engineering, Tianjin University, Tianjin 300072, China (J. Liang).

E-mail addresses: houf@tju.edu.cn (F. Hou), liangj@uow.edu.au (J. Liang).

¹ These authors contributed equally to this work.

Declaration of Competing Interest	417
Acknowledgements	417
References	417



Yuqing Wang is currently pursuing her bachelor's degree at the School of Materials Science and Engineering, Tianjin University. Her research interests focus on the design of new energy storage materials and the recycling of lithium-ion batteries.



Ning An is currently pursuing his bachelor's degree at the School of Materials Science and Engineering, Tianjin University. His research interests focus on carbon materials and new energy storage materials.



Prof. Feng Hou is the Director of the Institute for Advanced Ceramics at Tianjin University. He received his Ph.D. from the School of Material Science and Engineering, Tianjin University, China, in 2001. His research interests lie in the design of carbon nanotube-based films or fibers for energy storage applications and fabrication of fibrous porous ceramics for thermal protection systems.



Prof. Ji Liang received his Ph.D. from the University of Adelaide in 2014. After a T. S. Ke Fellowship and an ARC-DECRA fellowship, he joined the School of Materials Science and Engineering, Tianjin University. His research interests lie in the design of functional carbon-based materials for electrochemical catalysis and energy storage applications.



Lei Wen is an associate professor of Advanced Carbon Research Division at Shenyang National Laboratory for Materials Science, Institute of Metal Research, Chinese Academy of Sciences (IMR, CAS). He received his Ph.D. in Materials Science at North Eastern University, China, in 2004. His research interests focus mainly on lithium-ion batteries and flexible electrochemical energy storage devices.



Lei Wang obtained his master's degree at the School of Materials Science and Engineering, Tianjin University. His research interests focused on the structure design and doping process of novel electrode materials for lithium-ion batteries.



Xiaotong Jiang is currently working as a researcher in the Automotive Data of China Co., Ltd. He received his B.S in material science and engineering in 2015 and M.E in material engineering in 2018 from Tianjin University, Tianjin, China. His research interests are focused on the advanced carbon-based materials for high-performance energy-storage devices, such as lithium-ion batteries, supercapacitors, and so on.



Yuxin Yin received her Ph.D. from Tianjin University, China, in 2008. She is currently working as a senior engineer in Tianjin Lishen Battery Joint Stock Ltd Co, China. Her research interests include the production process and the recycling technology of lithium-ion batteries.

1. Introduction

With the rapid increase of population and the current development of the economy, there has been an urgent and significant demand for more sustainable and versatile energy supply. At this stage, about 85% of the energy around the world comes from non-renewable fossil fuels (e.g., oil, natural gas, and coal), which leads to aggravating energy crisis and environmental pollution [1,2]. With this regard, more sustainable and environment-friendly energy has been imposed with ever-increasing importance, which is typically harvested in the form of electricity from wind, solar, tidal, or hydraulic energies [3]. As a result of this, various types of batteries, especially lithium-ion batteries (LIBs), which store and release electricity via the reversible insertion and desorption of lithium ions in the electrode materials, have been intensively used and fabricated in a very large quantity [4–6].

Since their successful commercialization in the 1990s by SONY, LIBs have been widely applied in consumer electronic products, electric vehicles, and even grid-scale energy storage, due to their high energy density, non-memory-effect feature, and low self-discharge rate [7–11]. It has been reported that the production of new energy vehicles, only in China, has exceeded 1,250,000 in 2018 and will reach up to 2,000,000 by 2020 (Fig. 1a) [12,13]. This trend will not only lead to increased production of LIBs but also inevitably result in a large amount of the spent LIBs. It has been predicted that the total weight of the waste LIBs, only in China, would be over half a million tons in 2020 [14]. To make things even worse, owing to the short life span of the typical LIBs (i.e., 5 to 8 years), the first wave of retirement of LIBs, which were deployed

in EVs between 2008 and 2014, is approaching in the next few years. The number of waste LIBs in vehicles needed to be recycled can reach up to an optimistic value of 6.76 million in 2035 [15]. Therefore, it should be paid significant attention to the development of appropriate technologies for treating the spent LIBs and recycling the battery components, especially the elements that are low in reserve in the Earth crust.

Generally, a LIB is composed of a cathode, an anode, and a separator, which are immersed in the liquid electrolyte and sealed in the stainless steel, aluminum case or plastic pouch. The anode contains graphite powder as the active material, which is mixed with a binder, typically PVDF, and coated on a Cu foil current collector. On the other hand, the cathode may comprise different type of active materials, including lithium metal oxides or phosphides, such as LiCoO_2 (LCO) [16], LiMn_2O_4 (LMO) [17], $\text{LiNi}_x\text{Co}_y\text{Mn}_z\text{O}_2$ (LNCM) [18], $\text{LiNi}_x\text{Co}_y\text{Al}_z\text{O}_2$ (LNCA) [19], and LiFePO_4 (LFP) [20], which are coated on a Al current collector with carbon black as the conducting agent and PVDF as the binder. The mass percent of these cathode types in the LIBs market from 2016 to 2025 is shown in Fig. 1 (b) [21].

The rare elements, such as Co and Li in the cathode, have significant strategic importance and economic value. Due to the surge in LIB production, the price of cobalt has quadrupled from \$22 to \$81 per kilogram in the past two years [22]. With the rapid inflating of new energy vehicles market, the supply of these raw materials from natural resources will be unable to satisfy the future demand, unless properly recycled from the retired LIBs. On the one hand, a spent LIB contains considerable amounts of high-value elements: 5

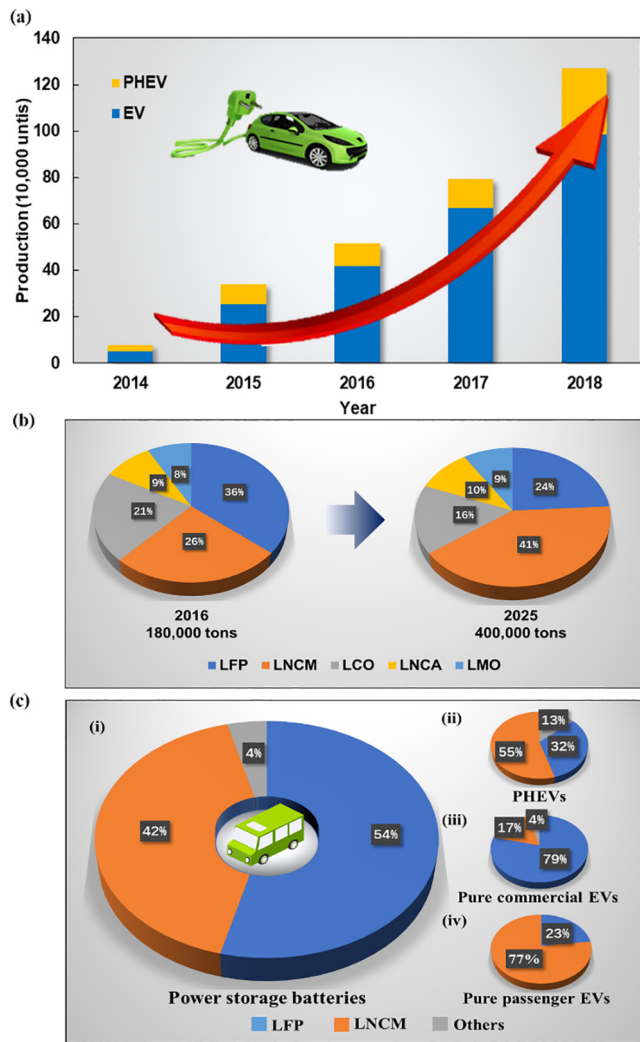


Fig. 1. (a) Pure electric vehicles (EVs) and plug-in hybrid electric vehicles (PHEVs) production of China from 2014 to 2018; (b) mass percentage of all LIBs market shares of the leading materials in 2016 and forecasted to 2025 [21]; (c) the percentage share of LFP and LNCM in (i) power storage batteries, (ii) PHEVs, (iii) pure commercial EVs and (iv) pure passenger EVs.

wt%–20 wt% of cobalt, 5 wt%–7 wt% of lithium, and 5 wt%–7 wt% of nickel, which is even higher than the natural ores [23–25]. Hence, the recycling of spent LIBs is a very feasible and economically viable approach to alleviating the urgent demand for raw materials. On the other hand, if disposed of improperly, the electrolytes (LiPF_6 and toxic organic solvents) and heavy metals, like Co, Mn, and Ni, in the spent LIBs will cause a serious environmental pollution and safety concern [26]. Therefore, the recycling of spent LIBs is extremely necessary regarding environmental protection and reuse of valuable resources.

Currently, LFP and LNCM are the two major cathode materials for LIBs, with the respective market share reaching 54% and 42% [27]. Besides, LFP and LNCM are the two most widely used batteries types in PHEVs and EVs that include pure commercial EVs and pure passenger EVs (Fig. 1c). When the capacity of a LIB decreases to 80% of its initial value, the battery is regarded to have reached the end of its life and cannot satisfy the requirements for EVs. When the battery retires, an industrial method of compromising the economic loss and continuing to make use of the remaining capacity value is “echelon utilization”. The “echelon utilization” includes two technical routes: the detection of the restructuring route and the battery repairing route [28]. In the detection of

restructuring routes, the spent batteries are detected and dismantled from the large arrays and modules into individual cells; then, the individual cells that are qualified for reuse are selected and constructed into new modules for reutilization. Detection is the key step in the reutilization process, which involves advanced and complicated technology; it becomes even more sophisticated owing to the differences in size and model of the retired batteries. In China, there are companies like Titan New Power Co., Ltd. and BYD Co., Ltd. that focus on the detection of restructuring technologies. In battery repairing routes, after the recovery of the solid electrolyte interface (SEI) and supplementation of new electrolyte, the spent LIBs are re-utilized in other applications that do not require high-performance batteries, such as low-speed EVs and backup power supply. Taking China Iron Tower company as an example, it began to purchase spent LIBs from EV companies, including BYD Co., Ltd., in 2018, and by the end of November 2018, this company has produced about 175,000 sets (450 MWh) of the echelon utilization batteries from the spent ones. After multiple testing procedures, these batteries are proven suitable for the communication base station. However, echelon utilization still faces technical barriers to recovery efficiency, safety, and reliability. More importantly, the recycled batteries will be exhausted after the long period of usage, anyway.

Apart from reusing the batteries, three major strategies have been developed to recycle the cathodic materials in LIBs, namely, pyrometallurgy, hydrometallurgy, and direct regeneration strategies.

Pyrometallurgy aims to recycle the metal elements from the spent LIBs in the form of metals or alloys. After dismantling the battery packs to individual cells, the batteries are directly treated in a high-temperature smelting furnace. The plastics, organic solvents, and graphite are burned to supply energy for the recycling process. Then the metal species like Co, Ni, and Cu are reduced to alloys with the aid of carbon reductant, while Li, Al, Si, Ca, and some of Fe reside in the slag [29,30]. Finally, the metals in the alloys can be separated through hydrometallurgical post-processing. As a simple method, pyrometallurgy has high technical maturity and has been adopted by some companies (e.g., Umicore) for the recycling of LIBs in consumer electronics. However, the valuable Li cannot be effectively recycled by this method, and other disadvantages, including the failure to recycle electrolyte, separator, and anode graphite, emission of hazardous gases, and high energy consumption also exist in this method, which is difficult to overcome. It is noteworthy that with the decreasing content of Co in the LIBs of EVs, pyrometallurgy may have poor economic viability when applied to the recovery of EVs' batteries [30,31]. At present, there are only very few reports about this method, so in this article, we do not discuss this in detail.

As for the hydrometallurgy method, it includes the leaching of metals into ions forms in solutions and subsequent recovery of these metals by selective separation into mono-metal products or into precursors for fabricating new electrode materials. In contrast to the pyrometallurgical method, the hydrometallurgical method is more widely applied for industrial-scale LIBs recycling and has been considered as an ideal approach with high recovery rates, low impurities, and good cost-effectiveness [32]. In China, Brunn Recycling Co., Ltd. and GEM Co., Ltd. are the representative companies implementing the hydrometallurgical methods and have achieved high recovering rates of over 98% for Ni, Co, Mn, and other metal elements.

Direct regeneration, on the other hand, is a novel strategy that “repairs” the cathode materials on the basis of the undamaged crystal structure through heat treatment, solid-state sintering, and hydrothermal methods. In the cathode of LIBs, significant Li loss and phase transformation often occur during prolonged cycling, which can be solved by direct regeneration. Generally, Li

loss is caused by the thickening of SEI film or the immobilized Li ions in the graphite anode; while the impurities or undesirable phase structure on the cathode materials is caused by the side reactions between the cracked cathode particles and electrolyte or the decomposition of the cathode materials. The direct regeneration treatment could effectively solve the above problems and restore the initial structure of the cathode materials [33–36].

Compared with the cathode materials recycling, the recycling of the anode materials of LIBs is often overlooked [37]. On the laboratory scale, researchers have been devoted to recovering the spent graphite as renewed anode, leaching lithium from the graphite, or further preparing other functional materials from the exhausted anodes [38–40].

Based on these latest developed strategies for recycling the LIB battery materials, we herein provide a brief review of these state-of-the-art recycling technologies for LIB materials, as shown in Fig. 2. As an overview of the whole work, the major technologies for recycling the LFP and LNCM cathode materials will be summarized. The advantages and disadvantages of the proposed methods will be presented and discussed. Afterward, we move on to the recent advances of the recycling technologies for graphite anode. Finally, the current challenges and the perspective solutions in recycling the battery components will be presented. We hope this review will not only provide a comprehensive illustration of the latest advances in this field but also shed light on the future development of novel battery recycling technologies to promote the environmental benignity and economic viability of the battery industry.

2. Recycling of the cathode materials

Recycling of cathode materials has both environmental and economic benefits. The whole recycling process of the cathode materials includes: (1) The pretreatment to separate the cathode active materials from other battery components and (2) the

hydrometallurgy or direct regeneration process to recover the valuable metal species from the cathode. Through the hydrometallurgy method, the microstructure of the cathode materials is completely destroyed to obtain the final products such as metal salts or high value-added precursors for fabricating new cathodes; while the direct regeneration method aims to repair the cathode materials based on their intact crystal structure.

2.1. Pretreatment of exhausted LIBs

The pretreatment process, including discharging, dismantling, and separating of exhausted LIBs and their components, is necessary for LIBs recycling to obtain different components. In the first step, the battery is fully discharged, by immersing it in a salt solution (e.g., NaCl solution), to avoid the short circuit caused by the remaining capacity [41–43]. Afterward, dismantling is carried out in a sealed environment for safety reasons, and the cathode plate, anode plate, separator, and battery packaging materials are obtained, respectively. Lastly, the battery active materials are separated from the current collectors, which is the key step during the pretreatment.

Since the cathode active material tightly adheres to the Al current collector by the PVDF or PTFE binder, it is not easy to be peeled off directly. Consequently, alkaline leaching [44–46], organic solvent dissolution [18,36,47–49], and thermal treatment [50–55] have been developed as the major ways in laboratory-scale studies to separate the cathode active material from the Al foil (Fig. 3).

Alkaline leaching is a common method in the separating process, which utilizes the solubility of Al in an alkaline solution [44–46]. In this process, a NaOH solution is typically used to dissolve the Al foil and isolate the cathode materials (Eq. (1)). Besides, using NaOH solution can also avoid the hydrolysis of LiPF₆, which will generate poisonous HF gas (Eq. (2)).

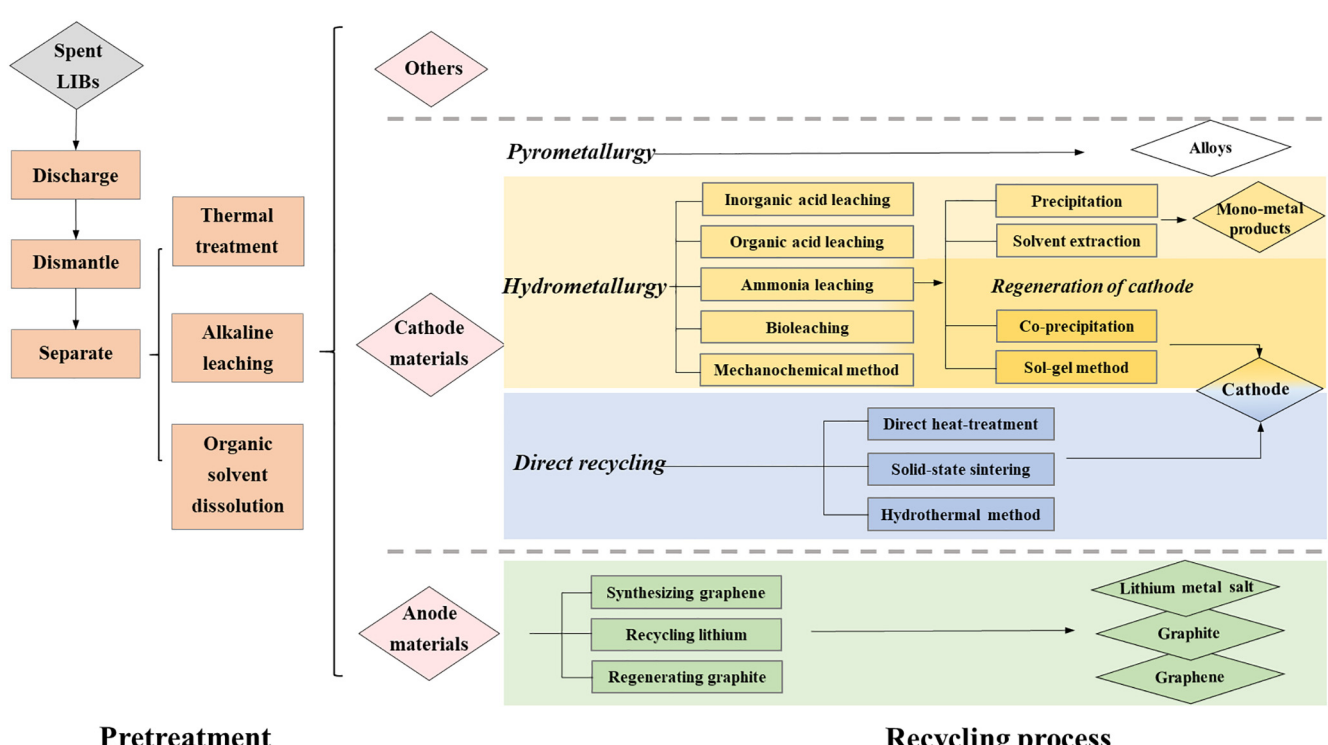


Fig. 2. Schematic illustration of typical recycling processes of spent LFP and LNCM batteries.

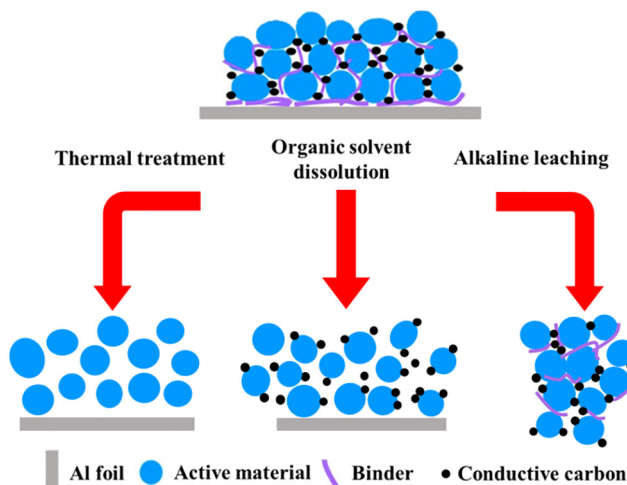


Fig. 3. Diagram of the process of separating the cathode material from the Al foil.

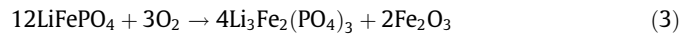


Nonetheless, this process causes the loss of Al and the obtained cathode material still need to be further calcined to remove the PVDF and conductive additives from it.

Apart from leaching the Al foil using the alkaline solution, the cathode active materials can also be separated from Al foil by dissolving the PVDF or PTFE binders using organic solvents. Song et al. demonstrated that the dissolution of the PVDF binder can be divided into three steps: (1) Solvent infiltrating into the electrode, (2) solvent reaching the PVDF adhesive and dissolving it, and (3) detachment of the cathode active materials [47]. They investigated the separation efficiency of different solvents, including *N*-methylpyrrolidone (NMP), acetone, *N,N*-dimethylacetamide (DMAC), and *N,N*-dimethylformamide (DMF), and found that DMAC was the most efficient and cost-effective one to dissolve PVDF. In contrast, for the nonpolarized PTFE binder, the polarized solvents cannot work well. Addressed at this, Zhang et al. adopted trifluoroacetic acid (TFA) to dissolve PTFE to strip the cathode materials from the Al foil [49]. Under the optimal conditions of a 15 vol% TFA aqueous solution, a liquid/solid ratio of 8.0 mL g⁻¹, and a reaction parameter of 40 °C for 180 min with proper agitation, the cathode materials could be completely separated. Owing to the acidity of TFA, however, some metal ions, such as Ni, Co, and Mn, can be dissolved as well. As a result, metal salts must be added as a composition for the cathode materials in the subsequent regeneration step, which might increase the cost of the recycling process. To further accelerate the dissolving process by organic solvents, additional treatment might be simultaneously incorporated. Sonication treatment is frequently adopted for this purpose due to its cavitation effect [56–58]. For example, Yao et al. combined the NMP dissolving and sonication to obtain the thoroughly separated cathode active materials [48]. Although the separation effect of organic solvent dissolution is good, however, the organic solvents are usually too expensive and environmentally harmful because of their toxicity.

Thermal treatment aims to burn out the binder at high temperature. As a simple and effective method, it can effectively weaken the adhesion between the cathode active material and the Al foil by removing the PVDF binder, which decomposes at ~350 °C [50–55]. Chen et al. heated the cathode at 300 °C for 1 h to decompose PVDF and further calcined the cathode powders at 550 °C for 0.5 h in air after crushing and sieving [50], at which temperature phase transformation from LiCoO₂ and LiMn₂O₄ to Co₃O₄ and Li₄Mn₅O₁₂ occurred, the binder and carbon additives were removed

completely, and the crystallinity of the particles also increased. It is worth mentioning that thermal treatment can oxidize Fe²⁺ to Fe³⁺, which is easier to be leached by acid for the recycling of LiFePO₄ [55,59], as described in Eq. (3).



Although poisonous gas, such as HF, is generated in the thermal treatment method, it is, however, still the most widely used in the industrial recycling process due to its simplicity and low cost. Recent research has demonstrated that the use of CaO during thermal treatment can eliminate the release of HF gas, which reduces air pollution and prolongs the service life of the high-temperature equipment [60].

2.2. Hydrometallurgical regeneration of the cathode materials

Hydrometallurgical regeneration aims to leach the pretreated cathode materials to ion forms in solutions and to separate metal ions to generate mono-metal salts, cathode materials, or other products. The hydrometallurgical process is considered as an ideal method for the recycling of spent LIBs due to the high recovery efficiencies, low impurity contents in the product, and low energy consumption of the process. Herein we illustrate hydrometallurgical recycling by two sections: (1) The leaching and separation of metal ions and (2) the regeneration of cathodes from the leachate.

2.2.1. Leaching and separation of metal ions

The leaching of the various valuable metal species from the cathode into a solution state is the key step during the hydrometallurgical process, because only in the solution state can the subsequent separation and recycling be conveniently achieved. According to the different leaching agents, leaching can be categorized into inorganic acid leaching, organic acid leaching, ammonia leaching, and bioleaching. The leaching method mentioned above should be assessed in comprehensive aspects, including leaching rates (the reaction speed of the leaching process), leaching efficiency (the ratio of the amount of ions in the leachate to the total amount of that species in the original cathode), environmental friendliness, price, and reutilization ability.

2.2.1.1. Leaching kinetics. Leaching is a chemical reaction acting between the liquid phase and the solid phase, which can be simply divided into five steps: (1) Leaching agents in the bulk solution diffuse to liquid–liquid interface, (2) leaching agents diffuse to solid active materials, (3) the leaching reaction proceeds on the interface of active materials particles, (4) the dissolved metal ions diffuse through the residual layer, and (5) the dissolved metal ions diffuse to the bulk solution, as shown in Fig. 4(a) [61]. Mainly, the speed of the leaching reaction is influenced by the mass diffusion and the chemical reaction, and the step in relatively lower speed (i.e. the speed-controlling step) determines the rates of the holistic leaching process. Therefore, in order to improve leaching rates, scholars have been studying the leaching kinetics to determine the speed-controlling step and to improve the reaction speed of this step, which in turn increases the whole leaching rates [62].

By far, two major theories have been developed to describe and explain the kinetics of the leaching process, namely, the shrinking-core model (Eqs. (4) and (5)) and Avrami equation model (Eq. (6)) [63,64].

$$1 - (1 - x)^{\frac{1}{3}} = k_1 t \quad (4)$$

$$1 - \frac{2}{3}x - (1 - x)^{\frac{2}{3}} = k_2 t \quad (5)$$

$$\ln[-\ln(1 - x)] = \ln k_3 + n \ln t \quad (6)$$

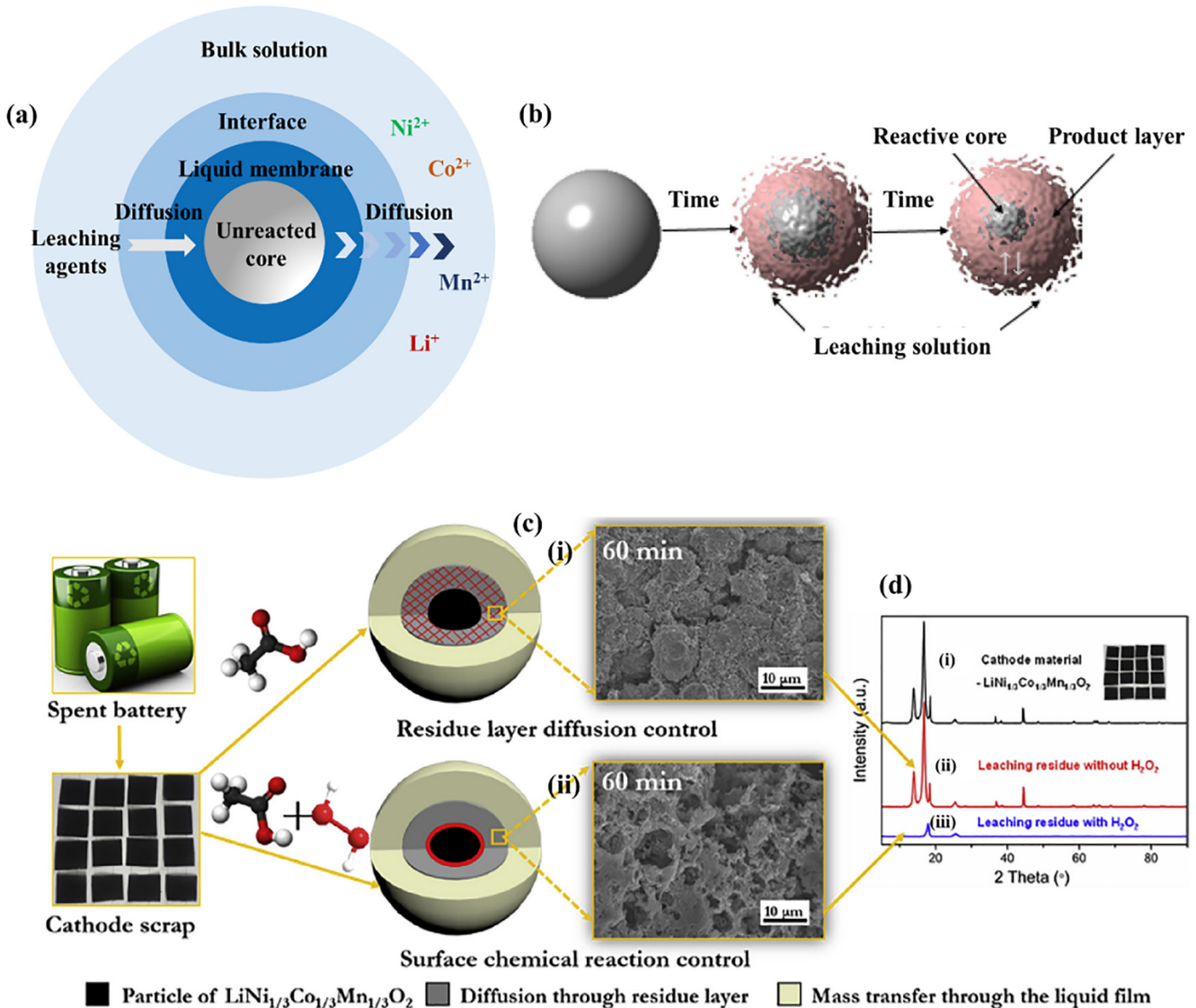


Fig. 4. (a) The diagram of the shrinking-core model [61]; (b) the illustration of the leaching process: the sphere solid materials remain unchanged [65]. (c) SEM images of the leaching residues without (upper) and with (lower) the addition of H_2O_2 after 60 min; (d) XRD patterns of cathode material- $\text{LiNi}_{1/3}\text{Co}_{1/3}\text{Mn}_{1/3}\text{O}_2$, leaching residue without the addition of H_2O_2 [66].

where x is the leaching efficiency of metals, k_1 , k_2 , k_3 are the reaction rate constants (min^{-1}), and t is the leaching time (min). Eqs. (4) and (5) represent the surface chemical control reaction and diffusion control reaction, respectively. Besides, the Arrhenius law can be applied to calculate the activation energy (E_a) of leaching reactions (Eq. (7)).

$$\ln k = \ln A - \frac{E_a}{R} \times \frac{1}{T} \quad (7)$$

where k is the reaction rate constant, A is the pre-exponential factor, E_a is the apparent activation energy, R is the universal gas constant, and T is the absolute temperature.

The shrinking core model is well suited to describe the leaching process because the leaching process meets the prerequisites of adopting the shrinking core model, which includes that solid active materials exist in a spherical shape, and volume of the sphere solid materials remains unchanged, as shown in Fig. 4(b) [65]. Thus, the shrinking core model is widely adopted to fit the relationship of x , and t tested from the leaching experiment and contributes to a more insightful understanding of the leaching process.

On this basis, Gao et al. studied the kinetics and efficiency of the leaching process with or without using the reductants. They reported that the existence of reductants could alter the speed-controlling steps in the leaching process from mass diffusion to chemical reaction [66]. In detail, in the absence of reductants, the high-valence metal ions, like Co^{3+} and Mn^{4+} , were inert and hard to be dissolved from the solid phase. As shown in Fig. 4(c), the residue layer was fairly dense, which acted as a barrier for mass diffusion and limited the leaching rate to the diffusion speed. Therefore, the $\text{LiNi}_{1/3}\text{Co}_{1/3}\text{Mn}_{1/3}\text{O}_2$ material maintained its original structure after the leaching. In contrast, when H_2O_2 was adopted as the reducing agent, the metal species were reduced to soluble +2 valence, and the dissolving of these metal ions caused the deterioration of the crystal structure of the original material, yielding a loose and porous structure that was composed of the binder and acetylene black (Fig. 4d). Such a loose structure had little restriction against the mass transfer. As a result, the introduction of H_2O_2 could not only speed up the overall leaching process and but also transfer the leaching manner from the diffusion-controlled to the chemical-reaction-controlled.

Moreover, He et al. studied the leaching kinetics of spent LNCM materials using a mixture of L-tartaric acid and H₂O₂ as the leachate and the reductant [67]. It was found that the overall leaching process can be divided into two stages, and the required E_a in the second stage for metal ions is lower than the first stage. Additionally, the leaching process in both stages followed the shrinking-core model, in which the actual leaching speed was controlled by the chemical reaction rate rather than the mass diffusion speed (Fig. 5a). Similarly, a two-step leaching process was also observed in the case of using D, L-malic acid and H₂O₂ [68]. Interestingly, different speed-controlling factors were identified for these two steps: the first step was controlled by the chemical reaction rate following Eq. (4), while the second step was diffusion-controlled that can be fitted by Eq. (5). It was also found that a different value of E_a is required for dissolving the metal species in the second stage. It can be attributed to the ash layer, which was formed during the initial leaching period and limited the diffusion of ions.

The Avrami equation, initially used to describe the process of crystallization, is also applicable to fit the leaching process. This is because the leaching process forms no products in the solid phase, and thus the leaching could be regarded as the reverse of

the crystallization [69]. On this basis, Zhuang et al. recently reported a mild leaching method using a mixture of phosphoric acid and citric acid (Fig. 5b). The leaching data conformed best with the Avrami equation (Eq. (6)) comparing with other equation, due to the decreased metal proportion in the solid phase during the leaching. Kinetics analysis revealed that the surface chemical reaction was the speed-controlling step during the leaching process.

2.2.1.2. Inorganic acid leaching and ion separation. Leaching using inorganic acids is a traditional leaching method for recycling LIBs, with a high leaching efficiency. The commonly used inorganic acids include HCl, H₂SO₄, HNO₃, and H₃PO₄ [32]. As mentioned above, this leaching process requires extra reducing or oxidant reagents when treating LNCMs or LFPs, respectively.

For the leaching of LNCMs, H₂SO₄ is the most widely used leaching agent in recent years, and the commonly used reducing agents are H₂O₂ [65,70,71], Na₂S₂O₅ [72], NH₄Cl [73], and glucose [74]. Vieceli et al. tested the leaching efficiency of H₂SO₄ coupled with different reducing agents, including Na₂S₂O₅, Na₂SO₃, H₂O₂, and iron scraps, as well as H₂SO₄ (Fig. 6) [72]. The results showed that the highest leaching efficiency for the transition metals (i.e., Co,

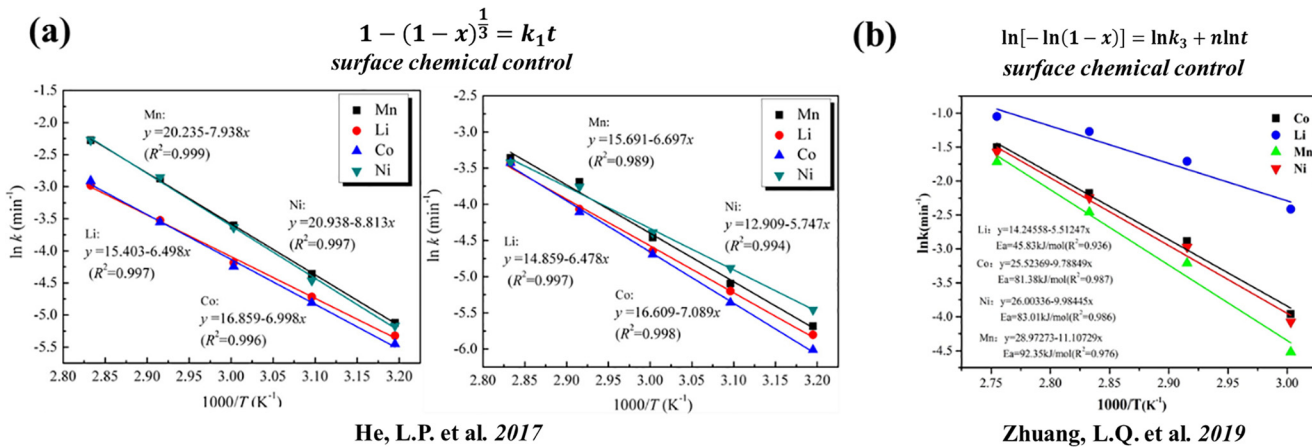


Fig. 5. Development of leaching kinetics analysis: Arrhenius plots for the leaching of Li, Ni, Co, and Mn based on (a) shrinking-core model controlled by surface chemical reaction with fast stage and slow stage [67]; (b) Avrami equation controlled by surface chemical reaction [69].

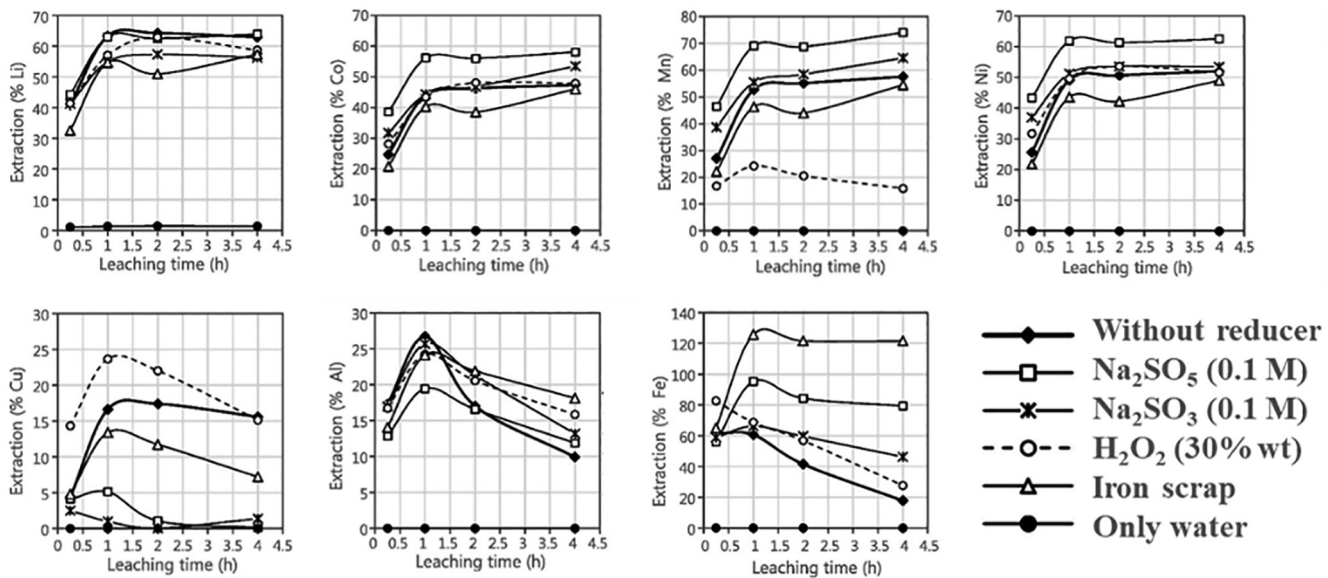


Fig. 6. Leaching efficiency of different metals from spent LNCM using different additives (leaching conditions: liquid/solid: 10 L kg⁻¹; 0.5 M of H₂SO₄; leaching temperature: 60 °C) [72].

Mn, and Ni) was achieved when using $\text{Na}_2\text{S}_2\text{O}_5$ as the reductant. In contrast, iron scrap showed the poorest extraction capability, except for Mn, for which the lowest leaching performance was associated with H_2O_2 , probably due to its difficulty in maintaining its soluble form (i.e., the Mn^{2+} ions) in the H_2O_2 medium. However, there have been other works reporting the satisfactory leaching efficiency of H_2O_2 for Mn, with a high efficiency up to 98.62%, by elaborately tuning the experiments parameters (i.e., leaching time of 90 min, temperature of 70 °C, acid concentration of 2.0 M, and H_2O_2 content of 10.0 vol%) [71].

Apart from different types of chemical reductants, the thermal reduction pretreatment has been applied for reducing the metal species as well, which avoids the usage of reducing agents in the typical leaching process. Additionally, thermal reduction can also lead to excellent leaching efficiency in the later leaching process, for Li, Ni, Co, and Mn up to 93.68%, 99.56%, 99.87%, and 99.9%, respectively, which are attributed to the complete deterioration of pristine layered structure to Ni, Co, NiO , and MnO phases [75]. The common reduction agents are carbon black [75] and the less expensive lignite [76].

After dissolving the valuable metals into ions in solution, separation of different metal species is required. Solvent extraction and selective precipitation are the two major metal ions separation methods. Solvent extraction is based on the uneven distribution of metal ions in the two-phase system (normally organic and aqueous phases) [62]. In this case, the most commonly used solvent extractants are Cyanex 272 for Co, D2EHPA for Mn, and PC-88A for Co and Ni. Besides, in the selective precipitation, Li, Co, Ni, and Mn can be precipitated from the solution phase in the form of Li_2CO_3 , Co(OH)_2 , CoC_2O_4 , NiCO_3 , and MnCO_3 , etc. [32].

A typical process of separating and recovering the metal products is schematically shown in Fig. 7(a) [70]. Potassium permanganate (KMnO_4), dimethylglyoxime ($\text{C}_4\text{H}_8\text{N}_2\text{O}_2$), and sodium carbonate (Na_2CO_3) are used as the precipitating agents for Mn, Ni, and Li, respectively; and Cyanex 272 is commonly used for the extraction of Co. Another typical protocol is shown in Fig. 7(b) [76], which includes the reduction roasting pretreatment. During the pretreatment, Li was transformed into Li_2CO_3 and could be separated by carbonated water leaching. Then Mn was extracted

by D2EHPA solution, while Co and Ni were sequentially extracted by PC-88A solution at different pH values. Finally, the sulfate products of NiSO_4 , CoSO_4 , and MnSO_4 were obtained after the evaporation of solvents.

For the hydrometallurgy method to recover LFPs, the most commonly employed leaching reagents are HCl [77,78], H_2SO_4 [26,79], and H_3PO_4 [80]. Different from the leaching process of LNCM material that requires the reducing agent, the pretreatment of LFP has to oxidize the Fe species from +2 to +3 valence state before the subsequent leaching and separation because the Fe^{3+} ions are more easily to form precipitants, like phosphate and hydroxide. The typical oxidation approach is to heat the LFP cathode at around 600 °C in the air [55] or using chemical oxidant agents, such as H_2O_2 or $\text{Na}_2\text{S}_2\text{O}_8$ [81].

For the LFP materials, on the other hand, two major strategies have been developed for their hydrometallurgical recovery, including the traditional method that dissolves both Li and Fe into ions forms and the novel method that selectively leaches Li while FePO_4 remains as the residue.

In the traditional strategy, after dissolving both Li and Fe to form an aqueous solution, the next key step is to separate Li^+ and Fe^{3+} ions. Commonly, selective precipitation of FePO_4 is achieved by heating the leachate [80] or adjusting pH values by adding NaOH [26] or ammonia [55,78]. Zheng et al. pointed out that the Fe/P molar ratio of the FePO_4 , which was recovered at a pH value of 1.9–2.1, was 0.961–1.008, with less than 0.005% impurities (Fig. 8a) [55]. Moreover, they also found that the PEG-6000 surfactant resulted in an ideal FePO_4 particle morphology with a smaller size and more uniform distribution than those obtained using other types of surfactants (Fig. 8b).

However, due to the very stable olivine structure of LFP, the traditional leaching process will consume an excessive amount of acid and alkaline to subsequently neutralize the solution. Apart from this, the separation of Li^+ and Fe^{3+} is also required in order to recover the valuable Li species from LFP. Therefore, to simplify and economize the process of recovering Li^+ , selective leaching of Li^+ with a reduced dosage of leaching reagents is essential [79,81]. Li et al. adopted H_2SO_4 with a strictly controlled amount. While the $\text{H}_2\text{SO}_4/\text{Li}$ molar ratio ranges from 0.33 to 0.57, the leach-

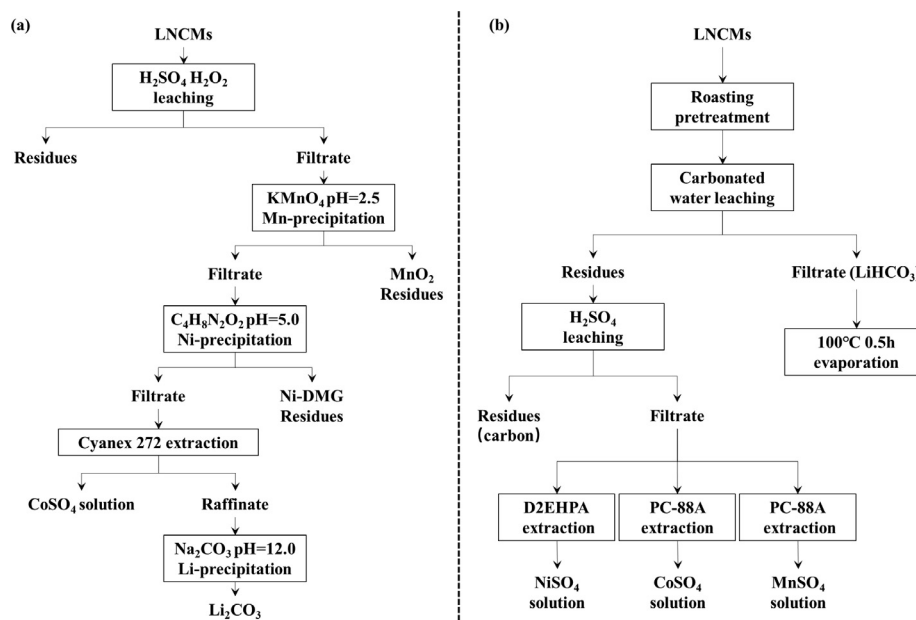


Fig. 7. The flowsheets for the recovery of valuable metals from spent LNCM (a) with extraction agents of Cyanex 272 [70]; (b) with extraction agents of D2EHPA and PC-88A [76].

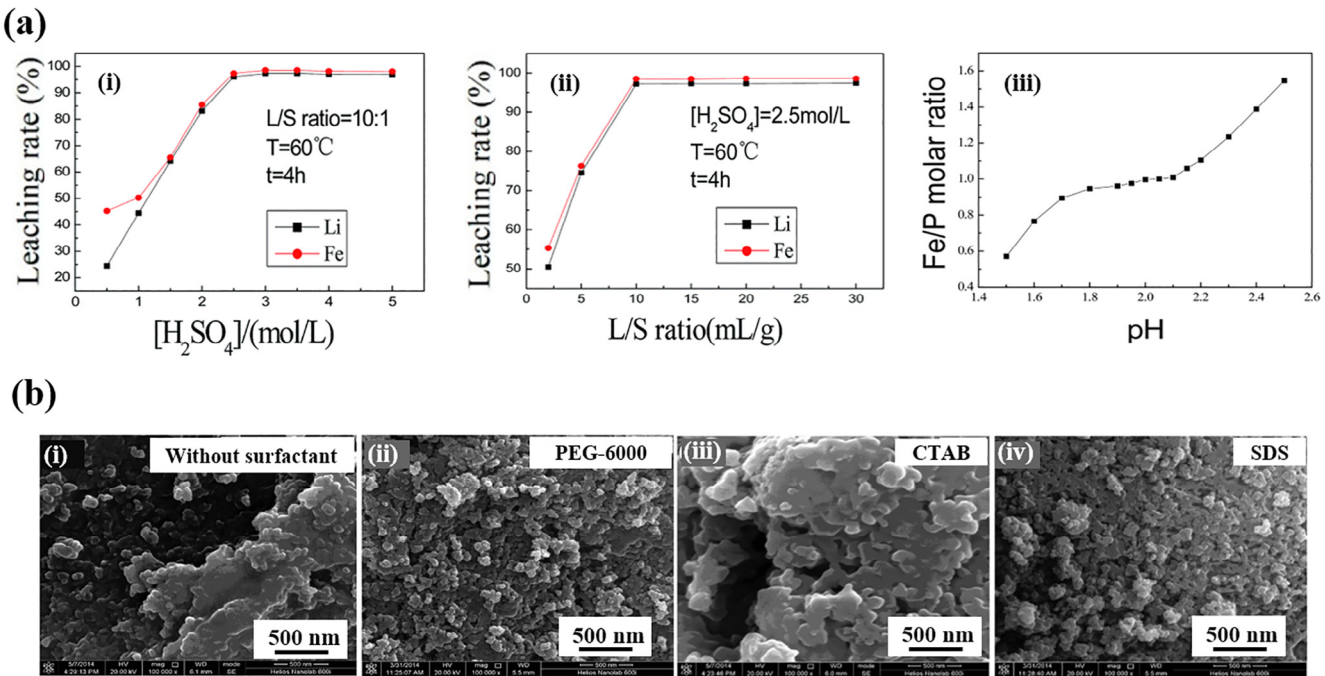
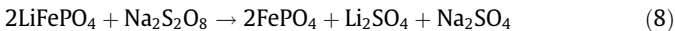


Fig. 8. In traditional strategy: (a) The effect of (i) H₂SO₄ concentration, (ii) liquid/solid ratio on the leaching efficiency of Li and Fe, (iii) the effect of pH value on the Fe/P molar ratio of recovered “FePO₄”; (b) SEM images of the recovered FePO₄·2H₂O: (i) Without surfactant, (ii) PEG-6000, (iii) CTAB, and (iv) SDS [55].

ing efficiency of Fe has no obvious change and a satisfactory leaching efficiency of 98.40% for Li⁺ was obtained (Fig. 9a, b) [79]. They also found that when the concentration of H₂SO₄ rose from 0.3 to 1.0 M (i.e., H₂SO₄/Li molar ratio rising from 0.55 to 1.82), the leaching efficiency of Fe would significantly increase from 0.0027% to 78.39%. As a result, to avoid the dissolution of Fe, the amount of H₂SO₄ has to be strictly controlled.

Besides, considering the low solubility of Li₃PO₄ in aqueous solution, Zhang et al. studied the selective leaching of Li to form highly soluble Li₂SO₄ using Na₂S₂O₈, which acted as both leaching and oxidant agent, following the conversion in Eq. (8) [81].



It was discovered that with a Na₂S₂O₈ dosage that was 1.05 times of the theoretical amount, the leaching efficiency of Li reached 97%, which was attributed to dissolving of Li ions into the aqueous solution while the crystal structure of regenerated FePO₄ could be maintained. After separating Li and Fe, Li can be recovered in the form of Li₂CO₃ or Li₃PO₄ precipitation and Fe can be recovered in the form of FePO₄.

In summary, the inorganic acid leaching and ion separation process possesses high leaching efficiency and recovery of metal products with high purity. However, the consumption of acid needs to be controlled and the optimal extraction parameter during the leaching process requires further optimization. The summary of the leaching/separation performance of current reports for LNCMs and LFPs using inorganic acid is shown in Table 1.

2.2.1.3. Organic acid leaching and ion separation. Though inorganic acids present excellent leaching performance, they will inevitably bring subsequent pollution issues, due to the usage of acerbic leachate, emission of harmful gases (such as SO₂, SO₃, NO_x), and other detrimental leaching residues. Consequently, the treatment and decontamination of these pollutions will be costly and a large quantity of water or alkaline will be consumed to neutralize the acidic leachate for the extraction of the valuable metals. Moreover, absorbing and purifying the by-produced gases also require devices like a cooler, condensation chamber, activated carbon fil-

ters, and bag filters [90]. Consequently, the inorganic leaching raises a whole series of environmental problems, which pushes the organic acids to be widely used as the more ideal and environmentally benign leaching agents.

Although the acidity of organic acid is relatively lower than the inorganic counterparts, some organic acids still show fairly good extraction efficiency in the leaching process, owing to not only the acidity to interact with cathode active materials but also the complexes formed between the metal cations in the active materials and the anions in the organic acids [91], which stabilizes the metal ions in solution. To better understand the leaching mechanism of organic acid by the formation of complexities, Li et al. studied the micro-scale coordination compounds formed from acetic acid or maleic acid with Li, Ni, Co, and Mn [92]. For the acetic acid, both monodentate and bridging coordination was formed, while only bridging coordination was formed in the case of maleic acid. They also studied the possible metallic complexes by Δ , which is an indicator of coordination reaction. Δ can be calculated from Eq. (9), which equals to the difference of asymmetric stretching vibration (ν_{as}) and symmetric stretching vibration (ν_s) of carboxylic acid.

$$\Delta = \nu_{as} - \nu_s \quad (9)$$

When Δ is less than 200 cm⁻¹, the coordinating mode tends to be bridging coordinate, and when Δ exceeds 200 cm⁻¹, the coordinating mode tends to be monodentate. The Δ values are 181, 116 cm⁻¹ for maleic acid and 135, 221 cm⁻¹ for acetic acid, respectively, revealing that maleic acid forms only bridging coordinate compounds with stable chelating performance; while acetic forms two types of compounds with metal ions: bridging coordination and the less stable monodentate coordination. The unstable chelating compounds tend to cause agglomeration and segregation of metal ions, resulting in impurities in the subsequent products. This study on metallic compounds is instructive for researchers to choose appropriate organic acids to leach and recycle metal ions.

Except for the molecular-scale explanation of the leaching mechanism, Li et al. also pointed out that the leaching process includes three sub-steps in macroscopic scale: particle loosening,

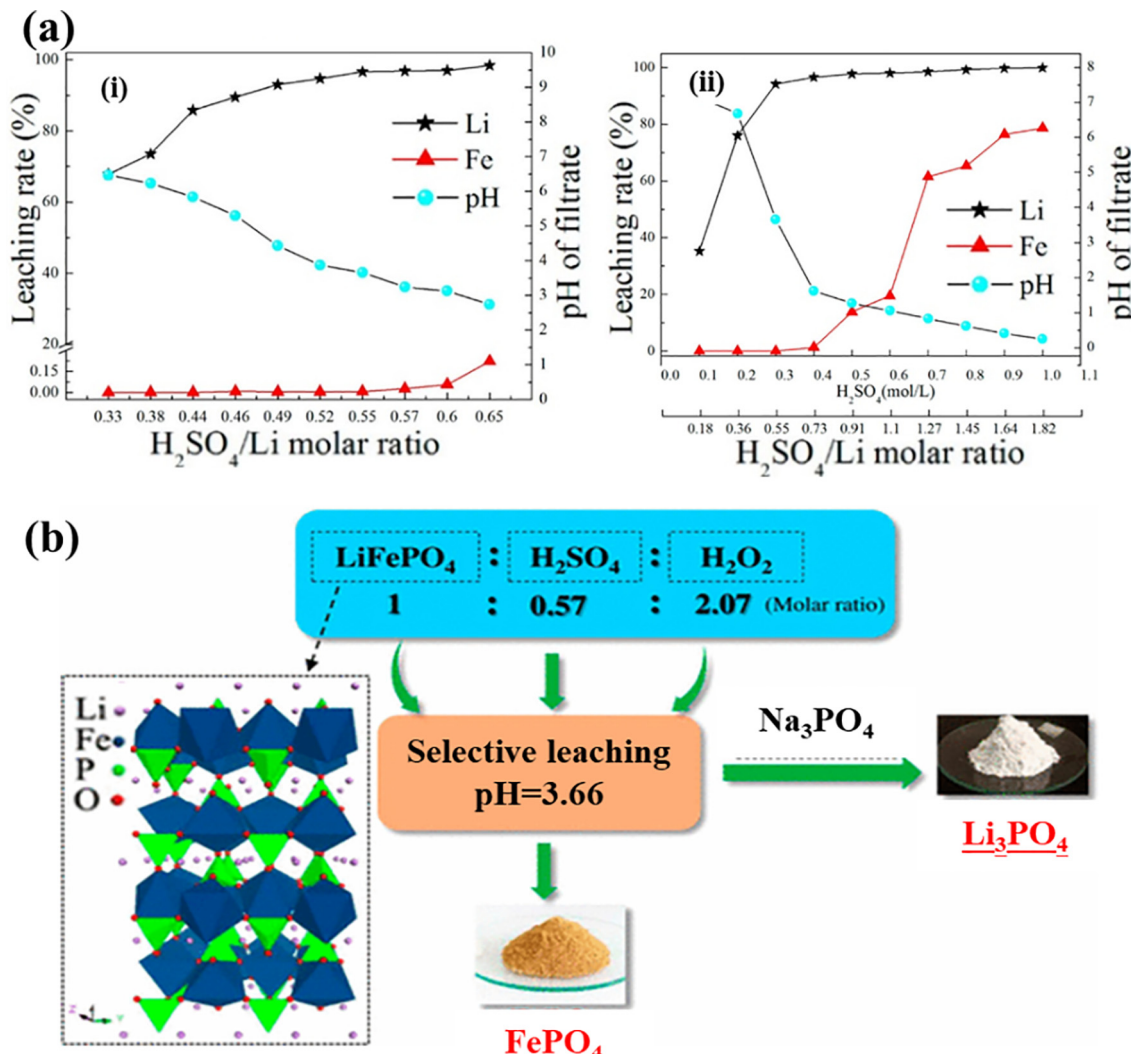
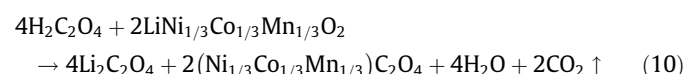


Fig. 9. In novel strategy: (a) The effect of (i) $\text{H}_2\text{SO}_4/\text{Li}$ molar ratio, (ii) H_2SO_4 concentration on the leaching efficiency of Li and Fe; (b) illustration of recovery of lithium, iron, and phosphorus from spent LiFePO_4 batteries using stoichiometric sulfuric acid leaching system [79].

breaking, and core shrinking, as shown in Fig. 10(a, b). Before leaching, the active material is an aggregation of spherical primary particles. In the initial few minutes of the leaching process, the large particles are loosened and broken. Afterward, in the core shrinking stages of primary particles, the macro-scale mechanism is another good conformation of the shrinking core model mentioned in 2.2.1a.

Apart from the acidity and chelating properties that are favorable for the leaching process, the organic acids also possess multiple other features, including precipitating and reducibility characters. By functioning as both the precipitant and leaching agent, the organic acid simplifies the process of leaching and metal ion separation into one step. For example, Sun et al. used oxalic acid as both the leaching agent and precipitant to recover cobalt in the form of CoC_2O_4 from the spent LiCoO_2 cathodic material [93]. However, this method is less practical for treating LNCM or other mixed cathode materials because oxalic acid can produce multiple precipitates in these cases, such as NiC_2O_4 , MnC_2O_4 , CuC_2O_4 , together with the desirable CoC_2O_4 product [32]. To avoid these impurities and reduce the separation complexity for obtaining the mono-metal salt products, a co-precipitate method was reported by Zhang et al. to separate metal Ni, Co, and Mn using oxalic acid, following Eq. (10), and the oxalate precipitates obtained by this

method can be further used as the precursor to re-synthesize new LNCM active materials. In this way, the leaching efficiencies of Ni, Co, and Mn can be over 98.5% and high value cathode products can be produced as well [94].



Moreover, organic acids also have the advantages of high stability and environmental friendliness as reductants. For example, Zhuang et al. used citric acid, which is more stable than H_2O_2 , to reduce metal from high valence states to lower ones [69]. Apart from this, other greener organic reductants, including cellulose, sucrose, and glucose, also have been proven suitable for the recycling of LiCoO_2 [95]. For example, Chen et al. used D-glucose as a reductant to recycle LNCMs. During the reductive leaching process, D-glucose was oxidized into H_2O and CO_2 with the formation of a sequence of eco-friendly organic acid intermediates, such as tartaric acid, formic acid, and oxalic acid [96]. Moreover, Pant et al. used natural citrus fruit juice, which comprised of citric acid, malic acid, ascorbic acid, and flavonoids, as both the leaching and reducing reagent [97]. By using this citrus fruit juice without other chemical reagents, the binder was successfully removed from the

Table 1

Summary of leaching results for LNCM and LFP in inorganic acid.

Cathode materials	Acid	Reducing agent for LNCM or oxidation agent for LFP	Leaching and recovery efficiency	Ref.
$\text{LiNi}_{1/3}\text{Co}_{1/3}\text{Mn}_{1/3}\text{O}_2$	H_2SO_4	H_2O_2	90% Mn and >96% Co	[82]
$\text{LiNi}_x\text{Co}_y\text{Mn}_{1-x-y}\text{O}_2$	H_2SO_4	/	92% Li, 92% Ni, 68% Co and 34.8% Mn	[70]
$\text{LiNi}_x\text{Co}_y\text{Mn}_{1-x-y}\text{O}_2$	H_2SO_4	H_2O_2	>98%	
$\text{LiNi}_x\text{Co}_y\text{Mn}_{1-x-y}\text{O}_2$	H_2SO_4	Carbon black roasting at 550 °C for 0.5 h	93.68% Li, 99.56% Ni, 99.87% Co, and 99.9% Mn	[75]
$\text{LiNi}_x\text{Co}_y\text{Mn}_{1-x-y}\text{O}_2$	H_2SO_4	Lignite roasting at 650 °C for 3 h	>80% Li, >96% Ni, Co and Mn	[83]
$\text{LiNi}_x\text{Co}_y\text{Mn}_{1-x-y}\text{O}_2$	H_2SO_4	$\text{Na}_2\text{S}_2\text{O}_3$	85% Li, 90% Ni, Co and Mn	[72]
$\text{LiNi}_x\text{Co}_y\text{Mn}_{1-x-y}\text{O}_2$	H_2SO_4	NH_4Cl	99.11% Li, 97.49% Ni, 97.55% Co, and 97.34% Mn	[73]
Mixed kinds of LIBs	H_2SO_4	H_2O_2	/	[65]
$\text{LiNi}_{1/3}\text{Co}_{1/3}\text{Mn}_{1/3}\text{O}_2$	H_2SO_4	H_2O_2	98.46% Co, 98.56% Ni, 99.76% Li and 98.62% Mn	[71]
$\text{LiNi}_{1/3}\text{Co}_{1/3}\text{Mn}_{1/3}\text{O}_2$	HNO_3 and HCl	/	71% Li, 33% Ni, 34% Co and 40% Mn	[84]
Mixed kinds of LIBs	H_2SO_4	H_2O_2	>97% Al, Mn, Ni, Co, and Li	[85]
$\text{LiNi}_x\text{Co}_y\text{Mn}_{1-x-y}\text{O}_2$	H_2SO_4	Reduction lignite roasting at 650 °C for 3 h	84.7% Li, >99% Ni, Co and Mn	[76]
$\text{LiNi}_x\text{Co}_y\text{Mn}_{1-x-y}\text{O}_2$	H_2SO_4	H_2O_2	99.7% Li, Ni, Co, and Mn	[86]
$\text{LiNi}_x\text{Co}_y\text{Mn}_{1-x-y}\text{O}_2$	H_2SO_4	H_2O_2	98% Ni, 99% Co and 84% Mn	[54]
Mixed kinds of LIBs	H_2SO_4	/	93.4% Li, 66.2% Co, 96.3% Ni and 50.2% Mn	[87]
Mixed kinds of LIBs	H_2SO_4	NaHSO_3	96.7% Li, 91.6% Co, 96.4% Ni and 87.9% Mn	[88]
LiFePO_4	/	$\text{Na}_2\text{S}_2\text{O}_3$	>99% Li	[81]
LiFePO_4	H_3PO_4	/	97.67% Fe and 94.29% Li	[89]
LiFePO_4	H_2SO_4	H_2O_2	96.85% Li	[79]
LiFePO_4	H_2SO_4	Heating at 600 °C for 1 h	98% Fe and 97% Li	[55]
LiFePO_4 and LiMn_2O_4	HCl	H_2O_2	80.93% Li, 85.40% Fe and 81.02% Mn	[77]
LiFePO_4	H_3PO_4	/	>95% Li and Fe	[80]
LiFePO_4	HCl	Heating at 700 °C for 10 h	/	[78]
LiFePO_4	H_2SO_4	H_2O_2	/	[26]

cathodic active materials and high leaching efficiencies of 100% for Li, 98% for Ni, 94% for Co, and 99% for Mn were achieved, respectively. More importantly, the organic acid leaching process also presents environmental friendliness because the organic acid presents a biodegradable nature and no secondary pollutions are generated. Recently, a recycling strategy of organic acid has been reported that the residual leaching agents could be re-utilized as leachate after metal ions are extracted [96].

In summary, the leaching performance of organic acid can be satisfactory in laboratory-scale, and the summary of leaching results for LNCMs and LFPs is shown in Table 2. However, the practical utilization of organic acids at the industrial scale to recycle LIBs has to be further explored, due to the relatively high price of the organic acids and the immaturity in the understanding of the complicated leaching mechanism with the organic acids.

2.2.1.4. Ammoniacal leaching. Besides the widely applied acid leaching, using ammonia-based agents to leach and separate metal ions from spent LIBs, especially LNCM, has been a hotspot in research in recent years [50,103–105]. The ammonia leaching possesses chelating characteristics, as shown in Eqs. (11) and (12) [106].



The unique advantage of this method lies with the chelating features of NH_3 , which can be utilized for selectively leaching the metal ions to separate Mn^{2+} from Ni^{2+} and Co^{2+} ions. Though transition metals present very similar properties, it has been proven that the ammonia-based agents tend to more easily dissolve Ni^{2+} and Co^{2+} ions rather than the Mn^{2+} ions. This selective leaching behavior can be attributed to the different solubility and stability of the as-formed complex with ammonia ligands. The $[\text{Co}(\text{NH}_3)_n]^{2+}$ complexes are soluble in the pH range of 9–11 and the $[\text{Ni}(\text{NH}_3)_n]^{2+}$ complexes are soluble in the pH range of 8.5–10.5. In contrast, the ligand of Mn^{2+} with ammonia is unstable in such conditions and tends to precipitate in the form of carbonates or oxides [106,107].

In a typical example, Ku et al. applied leaching agents, including ammonia ($\text{NH}_3\text{-H}_2\text{O}$), ammonium carbonate ($(\text{NH}_4)_2\text{CO}_3$), and ammonium sulfite ($(\text{NH}_4)_2\text{SO}_3$) to leach the LNCM cathode active materials. $(\text{NH}_4)_2\text{SO}_3$ served as the reductant and $(\text{NH}_4)_2\text{CO}_3$ served as the pH buffer. The pH variation was controlled within 0.2 around 8.3 in the pH buffering test, which is suitable for the existence of $[\text{Co}(\text{NH}_3)_6]^{2+}$, $[\text{Ni}(\text{NH}_3)_6]^{2+}$, and $[\text{Cu}(\text{NH}_3)_4]^{2+}$ complexes. The equilibrium constants were 1.3×10^5 for $[\text{Ni}(\text{NH}_3)_6]^{2+}$ and 5.5×10^8 for $[\text{Co}(\text{NH}_3)_6]^{2+}$. Due to the low equilibrium constant of Ni^{2+} complexes, the highest leaching efficiency of Ni (37%) is much lower than Co (94%). Zheng et al. adopted a similar two-step ammonia leaching process, which used $\text{NH}_3\text{-H}_2\text{O}$ as the leachate, ammonium sulfate ($(\text{NH}_4)_2\text{SO}_4$) and sodium sulfite (Na_2SO_3) as the reductant. In this method, the residue from the first leachate was continuously leached in the second step and a higher leaching efficiency for Ni^{2+} ions was achieved [104]. The leaching efficiencies in the first-step are 89.8% for Ni, 80.7% for Co, and 95.3% for Li, which increased to 94.8% for Ni, 88.4% for Co, and 96.7% for Li in the second leaching step. The improved leaching efficiency was attributed to the different composition of the leaching agents and different pH values (around 10.5) in the two steps.

For this method, however, the sulfite-based reducing agent is detrimental to the environment, due to the wastewater production. To avoid this, Wang et al. reported a thermal reduction pretreatment instead of using the sulfite reducing agent [105]. This pretreatment uses carbon as the reductant to reduce $\text{LiNi}_{0.5}\text{Co}_{0.2}\text{Mn}_{0.3}\text{O}_2$ into Ni, Co, MnO , and Li_2CO_3 . In this case, the leaching agents were sulfite-free, containing only $\text{NH}_3\text{-H}_2\text{O}$ and ammonium hydrocarbonate (NH_4HCO_3), and H_2O_2 was subsequently applied to oxidize the metallic Ni and Co to +2 valence ions to chelate with ammonia, forming soluble complexes in the leaching liquid. In this report, they recovered 81.2% of Li, 96.4% of Ni, and 96.3% of Co into Li_2CO_3 , NiSO_4 , and CoSO_4 products, respectively. Besides, the NH_4^+ ions could also be recycled through the ammonia distillation for further utilization, which achieved closed-loop recycling, as shown in Fig. 11.

On the other hand, ammonia is also commonly used to assist the precipitation of metal ions due to its alkalinity and chelating properties, which can modify the morphology and tap density of as-prepared precipitants as well [108]. For example, Liu et al.

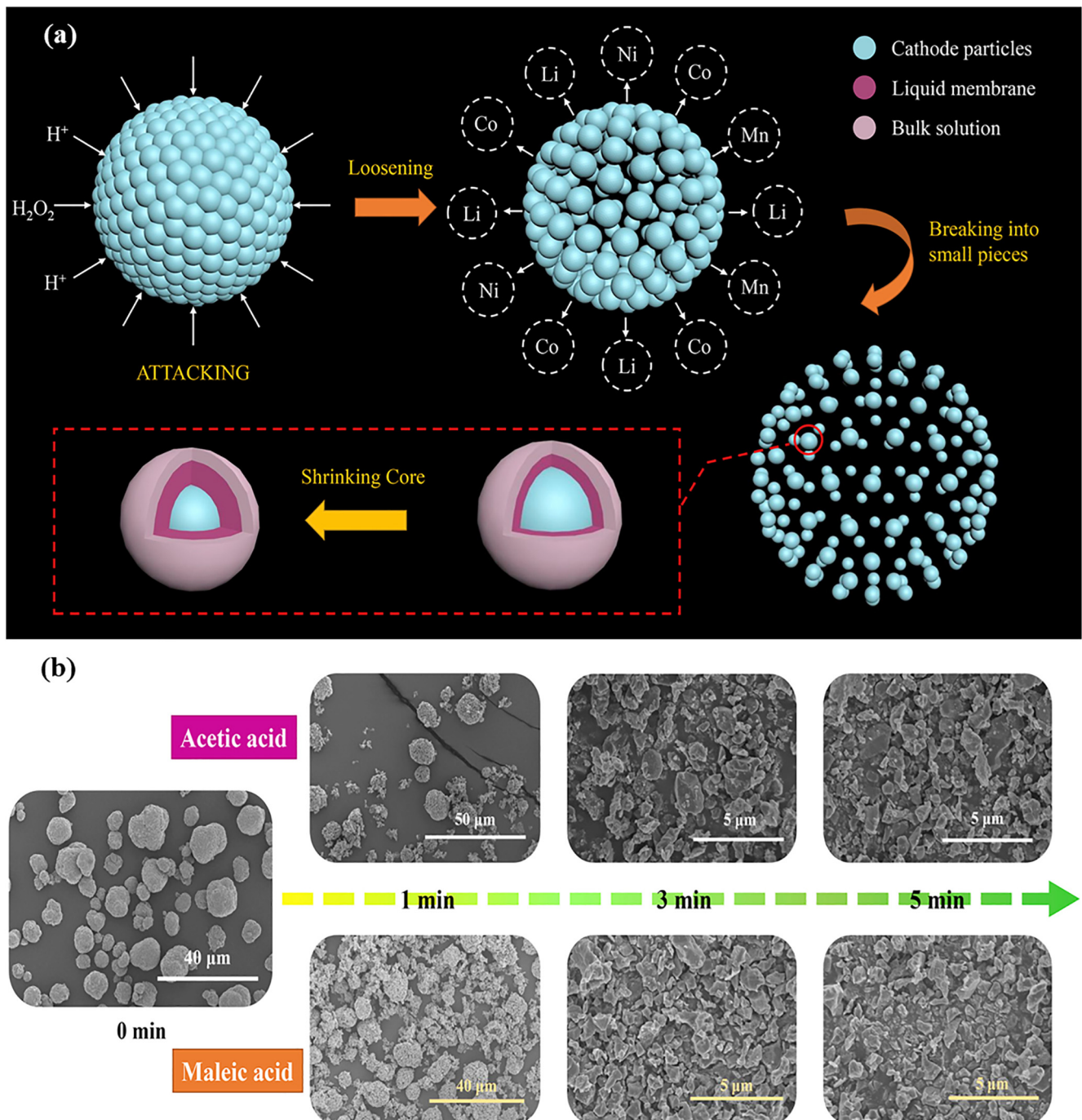
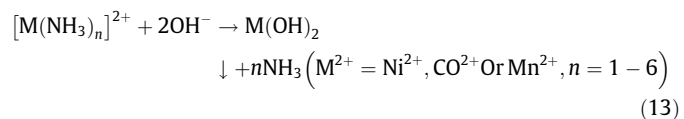


Fig. 10. (a) The diagrammatic sketch of reaction mechanism in the leaching process and (b) SEM images of residual powders in acetic acid and maleic acid leaching process [92].

obtained the $Ni_{1/3}Mn_{1/3}Co_{1/3}(OH)_2$ precursor from metal ammines, through the process shown in Eq. (13) [109].



Besides, He et al. recently reported a co-precipitation process to treat the LNCMs leachate, in which ammonia was added to control the nucleation and crystal growth during precipitation of $Ni_{1/3}Mn_{1/3}Co_{1/3}CO_3$, by utilizing the chelating capability of ammonia with metal ions [95]. As a result, homogeneous spherical particles with a narrow particle size distribution were obtained.

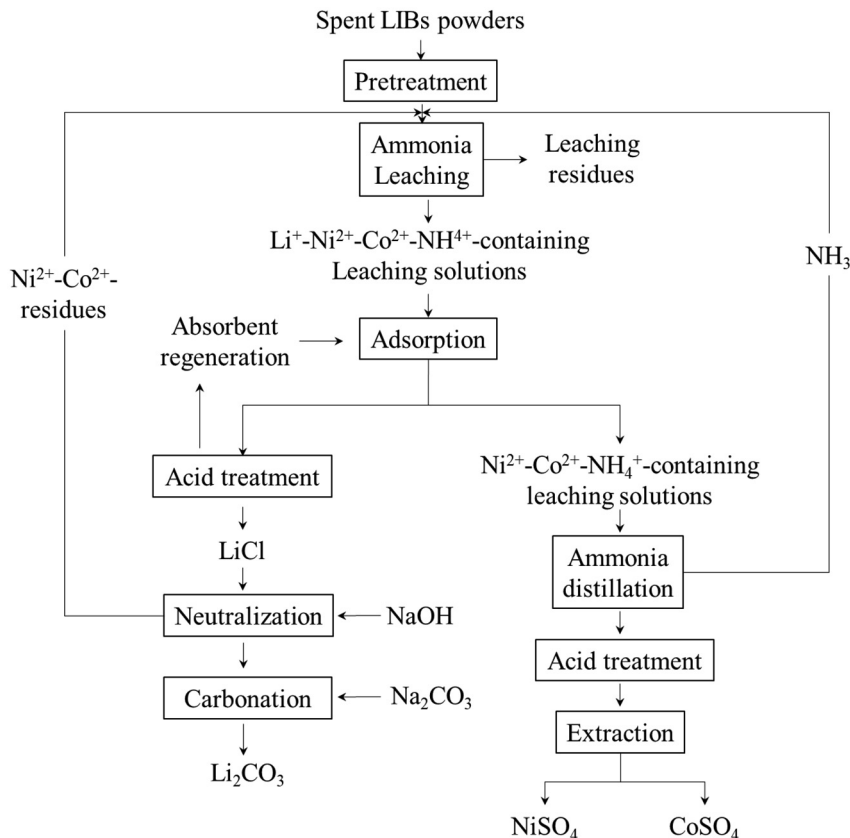
In summary, apart from being used as a separation agent for metal ions in the various leachate, ammonia also has been used as a substitute for acids for converting the metal species in the spent LIBs into ion forms in solutions. Importantly, ammonia-based leaching is also promising for closed-loop recycling, in which the ammonia from used leaching agents can be recycled for reuse by ammonia distillation, giving this process unique environmental friendliness [105].

2.2.1.5. Bioleaching. The bioleaching method utilizes the metabolites of microorganisms (e.g., bacteria and fungi) to recover metals from the spent LIBs. During a bioleaching process, the bioleaching media with energy sources, proper pH value, and microorganisms

Table 2

Summary of leaching results for LNCM and LFP in organic acid.

Cathodic materials	Acid	Reducing agent	Leaching and recovery efficiency	Ref.
$\text{LiNi}_{1/3}\text{Co}_{1/3}\text{Mn}_{1/3}\text{O}_2$	Acetic	H_2O_2	>98% Li, Co, Ni, Mn	[92]
$\text{LiNi}_x\text{Co}_y\text{Mn}_{1-x-y}\text{O}_2$	Acetic	H_2O_2	99.97% Li, 92.67% Ni, 93.62% Co, 96.32% Mn	[66]
$\text{LiNi}_{1/3}\text{Co}_{1/3}\text{Mn}_{1/3}\text{O}_2$	Lactic	H_2O_2	97.7% Li, 98.2% Ni, 98.9% Co, 98.4% Mn	[63]
$\text{LiNi}_{1/3}\text{Co}_{1/3}\text{Mn}_{1/3}\text{O}_2$	Formic	H_2O_2	98.22% Li, 99.96% Ni, 99.96% Co, 99.95% Mn	[98]
$\text{LiNi}_{1/3}\text{Co}_{1/3}\text{Mn}_{1/3}\text{O}_2$	Malic	Electrochemical cathode reduction	100% Li, 99.87% Ni, 99.58% Co, 99.82% Mn	[64]
$\text{LiNi}_{1/3}\text{Co}_{1/3}\text{Mn}_{1/3}\text{O}_2$	Maleic	H_2O_2	>98% Li, Co, Ni, Mn	[92]
$\text{LiNi}_{1/3}\text{Co}_{1/3}\text{Mn}_{1/3}\text{O}_2$	D, L-malic	H_2O_2	/	[99]
$\text{LiNi}_{1/3}\text{Co}_{1/3}\text{Mn}_{1/3}\text{O}_2$	Oxalic	Oxalic	>98.5% Ni, Co, Mn	[94]
$\text{LiNi}_x\text{Co}_y\text{Mn}_{1-x-y}\text{O}_2$	L-tartaric	H_2O_2	99.07% Li, 99.31% Ni, 98.64% Co, 99.31% Mn	[67]
$\text{LiNi}_{1/3}\text{Co}_{1/3}\text{Mn}_{1/3}\text{O}_2$	Citric	D-glucose	99% Li, 91% Ni, 92% Co, 94% Mn	[95]
$\text{LiNi}_{1/3}\text{Co}_{1/3}\text{Mn}_{1/3}\text{O}_2$	Citric	H_2O_2	/	[48]
$\text{LiNi}_{1/3}\text{Co}_{1/3}\text{Mn}_{1/3}\text{O}_2$	Citric	H_2O_2	97% Li, 95% Ni, 94% Co, 99% Mn	[100]
Mixed-cathode Materials	Citric	H_2O_2	99.1% Li, 98.7% Ni, 99.8% Co, 95.2% Mn,	[61]
$\text{LiNi}_{1/3}\text{Co}_{1/3}\text{Mn}_{1/3}\text{O}_2$	Trichloroacetic acid	H_2O_2	89.8% Li, 93% Ni, 91.8% Co, 91.8% Mn	[101]
$\text{LiNi}_x\text{Co}_y\text{Mn}_{1-x-y}\text{O}_2$	Citrus fruit juice	Citrus fruit juice	100% Li, 98% Ni, 94% Co, 99% Mn	[97]
$\text{LiNi}_{0.5}\text{Co}_{0.2}\text{Mn}_{0.3}\text{O}_2$	Phosphoric acid	Citric	100% Li, 93.38% Ni, 91.63% Co, 92.00% Mn	[69]
LiFePO_4	Oxalic	/	99% Li, 94% Fe	[102]

**Fig. 11.** Flowsheet of the recovery by ammoniacal leaching of Li, Ni, and Co from the spent LIB powders [105].

are firstly prepared. The microorganisms used for bioleaching are mainly acidophilic bacteria or fungi. Typically, they produce acid (e.g., H_2SO_4 or organic acid) that can dissolve metal ions in the spent cathode materials, similar to the hydrometallurgy process. It is regarded as a prospective alternative to the conventional hydrometallurgical processes due to its lower cost and environmental benignity [110,111].

For the acidophilic bacteria, Xin et al. used the sulfur-oxidizing bacteria (SOB) and iron-oxidizing bacteria (IOB) to leach metal ions from LiFePO_4 , LiMn_2O_4 , and $\text{LiNi}_x\text{Co}_y\text{Mn}_z\text{O}_2$ from three different energy sources, including sulfur, pyrite, and mixed system, and the bioleaching mechanisms of Li, Ni, Co, Mn were investi-

gated in detail [112]. The maximum leaching efficiency of Li was found in the sulfur-SOB system. In this case, the leaching of Li was only affected by the concentration of H_2SO_4 released by the microorganisms, while the leaching of other high-valence Ni, Co, and Mn ions was controlled by both the content of H_2SO_4 and the reductive Fe^{2+} generated by IOB. By adjusting the pH value in this system, the extraction efficiencies of the metal species from the spent $\text{LiNi}_x\text{Co}_y\text{Mn}_z\text{O}_2$ were all over 95% in the mixed energy source system.

Compared with bacteria, fungi have the advantages of higher tolerance to toxicity and acids, as well as shorter lag period to be adjusted to the new environment and faster leaching rates

[32,113]. Horeh et al. firstly employed this strategy to leach spent mobile phone batteries using *Aspergillus niger* under various experimental parameters, like different sucrose concentration, initial pH, and inoculum size [114]. The results indicated that the highest metal recovery of Cu, Li, Mn, and Al were 100%, 100%, 77%, and 75%, respectively, at 2% pulp density (w/v, i.e., the concentration of the cathode materials in the system); and 64% for Co and 54% for Ni were achieved at 1% pulp density. In another report by the same group, the adapted *Aspergillus niger* was used to leach Li, Co, Mn, Ni, Cu, and Al from spent LIBs [115]. The adaptation process was completed by gradually exposing the *Aspergillus niger* to higher concentrations of heavy metal ions to let the fungi acquire the resistance to them. As a result, the adapted *Aspergillus niger* was able to produce much more organic acid and showed higher extraction efficiency for the metal species than the unadapted ones.

The toughest dilemma for cultivating microorganisms is that it is hard for bacteria to reproduce and survive in the environment with abundant and miscellaneous heavy metal ions. Moreover, the bioleaching process is time-consuming, which normally takes several days to complete. Hence it may still take a long way to go for industrial applications.

To sum up, in order to select a suitable leaching method, all the factors including leaching rate, leaching efficiency, environmental friendliness, price and re-utilization of the reagents should be taken into consideration comprehensively. The performances of these leaching processes are listed in Table 3.

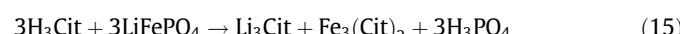
2.2.2. Mechanochemical-assisted metal leaching

The mechanochemical (MC) method uses the high-energy ball milling to initiate/accelerate the chemical reactions. It has been widely used for recycling metals from wastes, such as indium from used liquid crystal display panel [116], lead from cathode ray tube funnel glass [117], and rare earth elements from phosphors [118]. This unique method has also been applied for the pretreatment of the spent cathode materials to initiate reactions between cathode powders and reagents (e.g., chelating reagents), in which reduction of particle size, increase of specific surface area, decay of crystalline structure, and cleavage of chemical bond could simultaneously occur due to the large external energy introduced by the MC process. Consequently, the activation energy required for the metal extraction process decreases and reaction activity between the cathode active materials and leaching reagents increases [119], which are beneficial for improving the leaching efficiency of metal ions and reducing the acid consumption in comparison with the hydrometallurgy method [89,102,120–122].

Yang et al. proposed a closed-loop process for recycling Li and Fe from spent LiFePO₄ batteries by co-grinding LiFePO₄ with EDTA-2Na as the metal chelating reagent [89]. Using the diluted H₃PO₄ solution as the leaching agent, leaching efficiencies of 94.29% for Fe and 92.04% for Li were achieved, which were much higher than the un-ground samples (Fig. 12a) and could be attributed to the destruction of (311) plane during the MC process

(Fig. 12b, c). However, the cost of EDTA-2Na is high and the acid leaching can bring secondary pollution. Addressing at this, efforts have been made to use other low-cost organic acids or even avoid the acid leaching step. For example, Fan et al. achieved the selective extraction of Li and Fe by co-grinding the cathode powder with oxalic acid and deionized water prior to water leaching [102]. The MC process in this process could be divided into three stages: the reduction of particle size, the breaking of chemical bonds, and the generation of new chemical bonds (Fig. 12d). Under the optimized conditions, the extraction efficiency of Li reached 99.34%, which was much higher than the cases using acid leaching with or without milling pretreatment (Fig. 12e). In addition, they found that the wet MC process can lead to a higher Li extraction efficiency compared with the dry MC process, due to the absence of blind corners to result in a more thoroughly destroyed crystal structure of the cathode materials.

Besides, mild and eco-friendly citric acid was also used by Li et al. to grind with the LiFePO₄ materials [120]. When H₂O₂ was used as the oxidant, the extraction efficiency of Li reached 99.35%. However, Fe was hard to extract because Fe²⁺ ions were oxidized to Fe³⁺ under this condition and recovered as solid FePO₄ (Eq. (14)). In the case that H₂O was used instead of H₂O₂, Fe²⁺ can stably remain in the leachate in the form of Fe₃(Cit)₂ (Eq. (15)). As a result, both Li and Fe can be extracted from the cathode into the leachate, and the extraction efficiencies of Li and Fe were 97.82% and 95.62%, respectively. Hence adding H₂O₂ can help selectively recover Li and further separation of Fe²⁺ and Li⁺ ions can be avoided.



With improved extraction efficiency and less chemical agent consumption, the MC method has the potential to be scaled up for industrial applications [58].

2.2.3. Regeneration of cathode from the leachate

After dissolving the metal ions in the leaching agents, the next step is to obtain valuable products, i.e., the new electrode materials or their precursors, from the leachate. Traditionally, as mentioned above, the metal ions in the leachate are converted into insoluble mono hydroxides or salts precipitants [32]. The selective precipitation, however, is a tedious process including a sequence of steps to separate individual metallic ions. To simplify the complex steps, effective recovery strategies have been developed to directly regenerate cathode materials or their precursors from the leachate, in a more cost-effective and environmentally friendly manner to obtain the high-value products and achieve the closed-loop recycling of LIBs [62].

Co-precipitation is the most frequently adopted method to prepare the precursor of cathode materials, which uses the leachate containing multiple metal ions obtained from the hydrometallurgical leaching of the spent cathode materials. Then, the co-

Table 3

Summary of comparison between different leaching methods in leaching rates, leaching efficiency, environmental friendliness, price and reutilization ability.

Leaching methods	Performance				
	Leaching rates	Leaching efficiency	Environmental friendliness	Price of reagents	Reutilization of reagent
Inorganic acid leaching	••••	••••	•	•	•
Organic acid leaching	•••	•••	•••	•••	•••
Ammonia leaching	••	••	•••	•••	•••
Bioleaching	•	•••	••••	•	•

Best Worst.

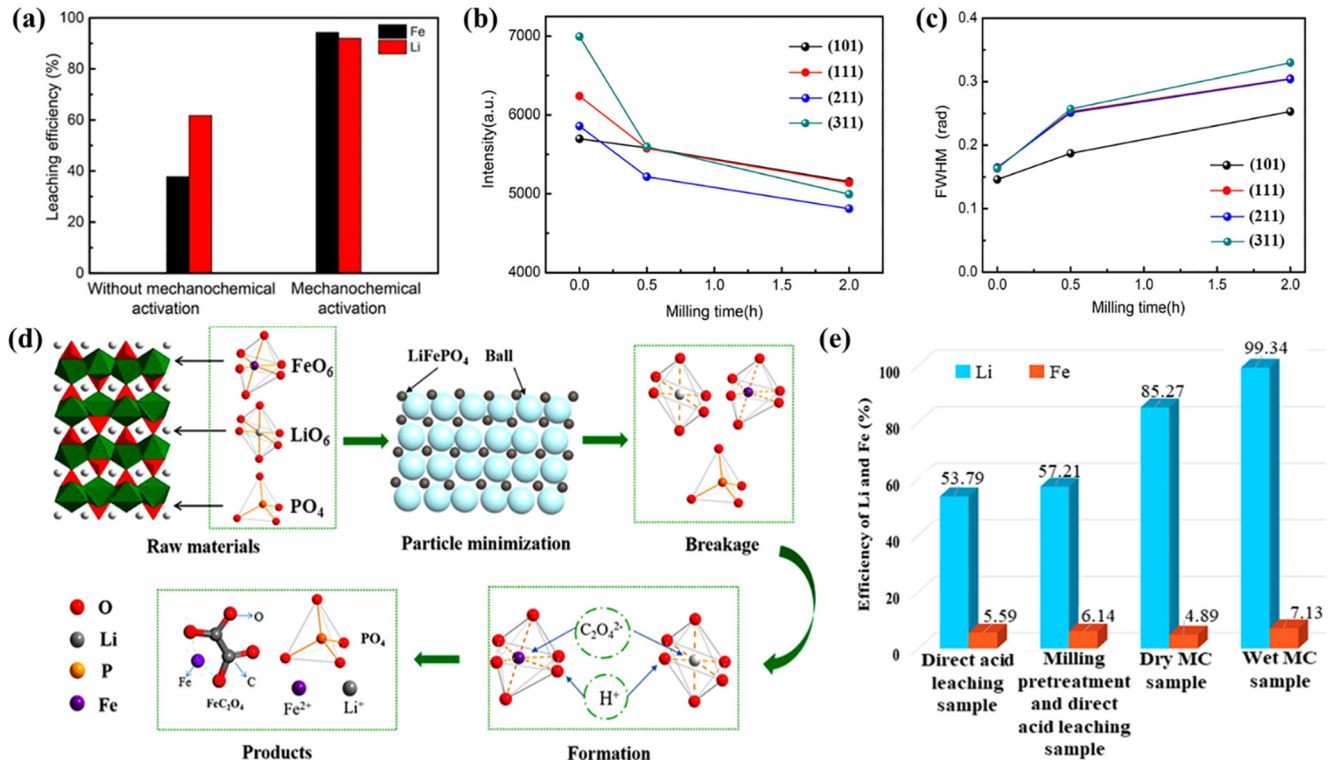


Fig. 12. (a) Leaching efficiency of Fe and Li from different samples (mechanochemical activation sample, activation time of 5 h, mass ratio of cathode powder to EDTA-2Na ratio of 3:1; leaching parameters: H₃PO₄ of 0.5 M, solid/liquid ratio of 40 g L⁻¹, and leaching time of 60 min); (b) X-ray diffraction intensity and (c) the full width at half-maximum (FWHM) of lattice planes with milling time [89]; (d) possible products and mechanism in the mechanochemical process; (e) extraction of Li and Fe from different samples. Conditions: grinding time of 2 h, rotation speed of 500 rpm, mass ratio of LiFePO₄ to oxalic acid of 1:1, ball to powder mass ratio of 20:1 [102].

precipitated precursor mixed with Li source (e.g., Li₂CO₃) was annealed to prepare the regenerated LNCMs. This strategy is state-of-the-art because it can avoid the complex steps to separate different metal ions, especially the metal species with similar characteristics like Ni, Co, and Mn. In this way, the leachate can be directly used for co-precipitation by adjusting the pH values and the mole ratio of metal ions. Recently, different types of precursors for fabricating cathode materials have been obtained by co-precipitation, including hydroxide, carbonate, and oxalate. For example, Sencanski et al. utilized the co-precipitation method to directly obtain Ni_{1/3}Mn_{1/3}Co_{1/3}(OH)₂ from the leachate and used it as the precursor to fabricate LNCM cathode material [123]. However, the as-prepared LNCM presented a low crystallinity and undesirable cation mixing, which is unfavorable for achieving high capacity for LIBs (Fig. 13a, b). Recently, Zheng et al. synthesized LNCM from a similar precursor prepared by the hydroxide co-precipitation process and obtained a uniform and steady precursor precipitant [124]. It was found the precipitating process could be divided into three stages, according to the different particle morphologies: the formation of small primary particles, the partial agglomeration to form secondary particles, and the formation of particles with uniform sizes. It was also found that the 48-hour precipitating was the best condition to allow the precipitation reaction to reach the steady-state for co-precipitation (Fig. 13c). The regenerated LNCM materials possessed excellent rate capability of 74.7 and 22.2 mAh g⁻¹ at 5 C and 10 C, respectively (Fig. 13d), which is even higher than the commercial LNCM material. The satisfactory electrochemical performance was attributed to the higher pore volume and higher porosity of the regenerated LNCM materials.

The above-obtained Ni_{1/3}Mn_{1/3}Co_{1/3}(OH)₂ precursor still faces some problems of instability because the Mn(OH)₂ precipitant

tends to segregate from the mixed hydroxide and be oxidized to MnOOH or Mn₃O₄ phases [125]. To avoid this, He et al. reported the co-precipitating of Ni_{1/3}Mn_{1/3}Co_{1/3}CO₃ to regenerate LNCM, because the MnCO₃ precipitate is more stable than the hydroxides [95]. Additionally, Zhang et al. also reported a partial co-precipitating method to convert only the surface of LNCM particles to oxalates by adopting oxalic acid as both leaching reagent and precipitant; while the Li element inside the particle was simultaneously dissolved, leaving an NCM oxide core. Consequently, the precursor obtained by this method has a core-shell structure, with an NCM core inside an oxalic acid precipitant (Ni_{1/3}Mn_{1/3}Co_{1/3}C₂O₄) shell (Fig. 14a) [94]. In the shell of the structure, the impurities like Co₃O₄ and NiCo₂O₄ were removed by oxalate and the oxalate layer was subsequently formed on the particle surface. While in the core of the structure, the pristine layered crystal structure of LNCM remained (Fig. 14a–c). As the leaching time prolonged, the NCM core gradually shrank and was converted to oxalates. The electrochemical testing shows that the LNCM regenerated from the precursor obtained by the 10 min leaching exhibited the best electrochemical performance with an initial discharge capacity of 168 mAh g⁻¹ and capacity retention of 91.5% after 150 cycles at 0.2 C (Fig. 14d). This excellent electrochemical performance was attributed to the well maintained α -NaFeO₂ structure of the LNCM active material inside the agglomerated particles (Fig. 14a, e).

Sol-gel regeneration has also been developed to resynthesize the cathodic active materials from the leachate produced from the organic acid leaching process [61,126], in which the organic acid simultaneously acts as the chelating reagents. Therefore, the sol-gel process requires no extra chelating reagents, making it economically viable to some extent. The typical process of sol-gel regeneration is shown in Fig. 15(a) [63]. After the acid leaching, extra metal salts and aqueous ammonia are added to the leachate

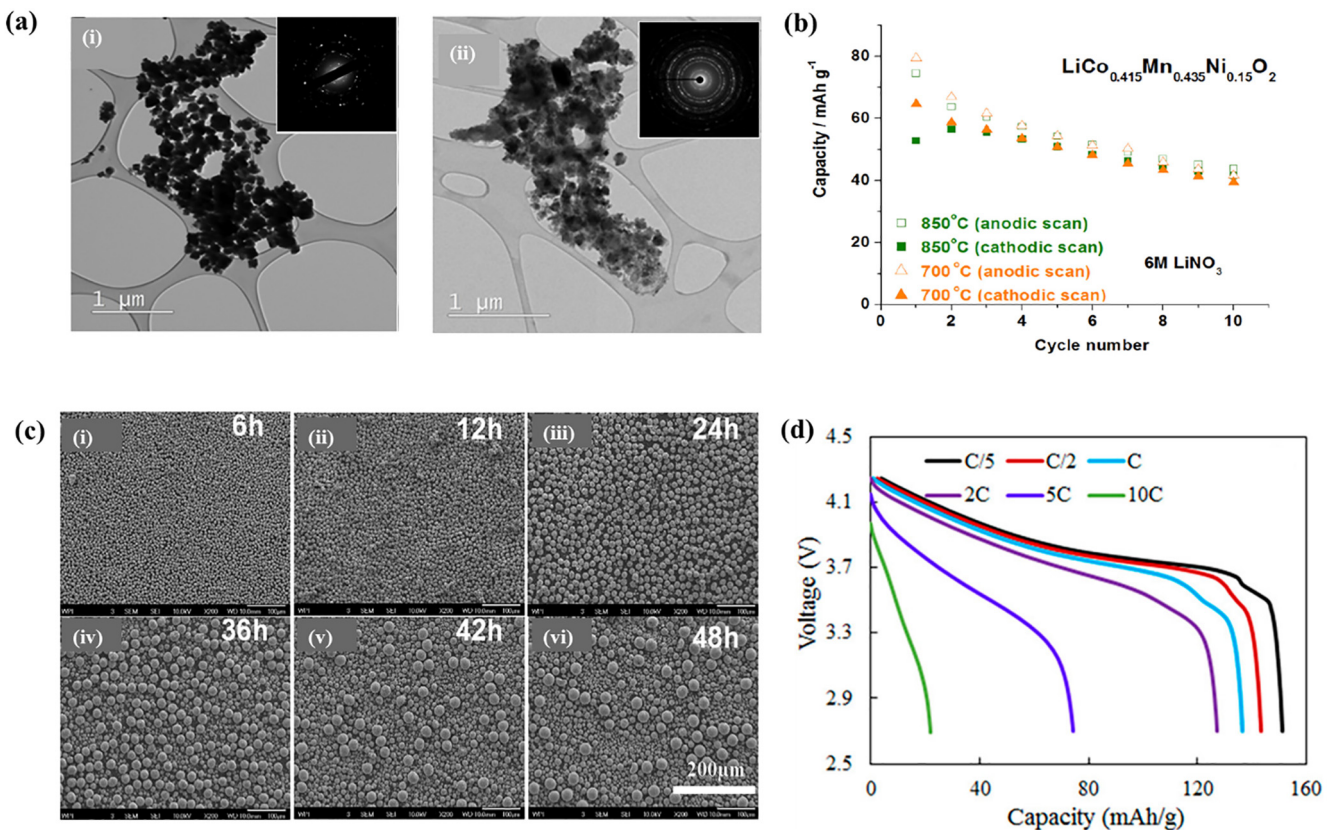


Fig. 13. (a) TEM of $\text{Li}(\text{Ni}_{1/3}\text{Mn}_{1/3}\text{Co}_{1/3})\text{O}_2$ (i) calcined at $850\text{ }^\circ\text{C}$ and (ii) calcined at $700\text{ }^\circ\text{C}$; (b) the corresponding charge/discharge capacity [123]. (c) SEM images of $\text{Ni}_{1/3}\text{Co}_{1/3}\text{Mn}_{1/3}(\text{OH})_2$ as a function of reaction time of (i) 6 h, (ii) 12 h, (iii) 24 h, (iv) 36 h, (v) 42 h; and (vi) 48 h; (d) discharge curves of #1NMC at various rates [124].

solution to adjust the mole ratio of Ni:Co:Mn and pH value. Then the solution was heated to remove water and the transparent gel was obtained. The gel was calcined to decompose the organic components and the precursor was formed. Compared with the coprecipitation method, the particle size of the precursor obtained by the sol-gel method or the subsequently resynthesized cathode materials is smaller ($<1000\text{ nm}$) and more uniform [99]. Besides, the calcination conditions of sol-gel precursors to resynthesized LNCM have been studied in detail. By changing the annealing temperature, the crystallinity and layered structures of the obtained materials could also be modified (Fig. 15b). Specifically, the samples obtained at a higher temperature (850 or $950\text{ }^\circ\text{C}$) had a better-ordered layered structure and crystallization than the counterpart obtained at $750\text{ }^\circ\text{C}$. In these analogs, the one obtained at $850\text{ }^\circ\text{C}$ reached the highest initial capacity of 147.2 mAh g^{-1} at 0.5 C and better cycling performance as well (Fig. 15c). Besides, the resynthesized cathode materials obtain an excellent crystalline structure of faceted, edge-blunted polyhedral and regular octahedral structure (Fig. 15d) instead of the secondary aggregation comprised of small particles. This well-ordered crystal structure shows great potential for preparing single crystal cathode from spent LNCMs. On the other hand, the sol-gel regeneration can be obtained with another organic acid (e.g., lactic acid and citric acid) and the resynthesized LNCM also exhibits excellent crystal structure and electrochemical performance (Fig. 16a-d) [63].

Generally, the regeneration of LNCM cathode materials has great economic and environmental potentials and a systematical summary of the regeneration approach of cathode materials from spent LIBs is shown in Table 4. In order to convert the laboratory method to large-scale recycling line in a factory, great efforts should be paid to explore a more universal recycling strategy, in which different kinds of LIBs (LCO, LMO, NCM, LFP) can be recycled

in one batch and the required labor can be minimized [61]. For this purpose, Zheng et al. have developed a recycling method that is indiscriminate of the different types of spent LIBs [124]. In this study, cathode precursors in a hydroxide form were recovered from four different disassembling lines of spent LIBs with different chemical compositions, and they exhibited little differences in morphology, particle size distribution, and tap density (Fig. 17). The regenerated particles are uniformly dispersed and the sizes of the secondary particles are around $10\text{ }\mu\text{m}$ with the tap densities of around 2.5 g cm^{-3} , which meets the requirement for high-end Li-ion battery industrial manufacturing. Besides, this method of hydroxide co-precipitation regeneration has also been reported applicable to recycle Ni-rich LNCMs with satisfactory initial discharge capacitance of 197.7 mAh g^{-1} for $\text{LiNi}_{0.8}\text{Co}_{0.1}\text{Mn}_{0.1}\text{O}_2$ and 174.3 mAh g^{-1} for $\text{LiNi}_{0.5}\text{Co}_{0.2}\text{Mn}_{0.3}\text{O}_2$ [124]. Therefore, the hydroxide co-precipitation method is highly promising in industrial-scale applications due to the competence of recycling mixed kinds of LNCMs and, in turn, regenerate LNCMs with higher capacitance and energy density.

As for LiFePO_4 , the thermal reduction method is a typical method to regenerate it. The recovered $\text{FePO}_4 \cdot 2\text{H}_2\text{O}$, which was prepared by the solution-precipitation method as the Fe and P precursor, was calcined with Li precursor (e.g., Li_2CO_3) in the presence of carbon or carbonaceous reductant [79,80] to obtain the LiFePO_4 cathode material. In this case, the quality of the $\text{FePO}_4 \cdot 2\text{H}_2\text{O}$ precursor largely determines the actual performance of the finally obtained LiFePO_4 . For example, by using the recovered $\text{FePO}_4 \cdot 2\text{H}_2\text{O}$ and commercial Li_2CO_3 as the precursors and glucose as the reductant, a LiFePO_4/C composite with a hierarchical microflower structure was successfully synthesized [80]. It exhibited good performance as a LIB cathode material with a discharge capacity of 159.3 mAh g^{-1} at 0.1 C and a 95.4% capacity retention after 500

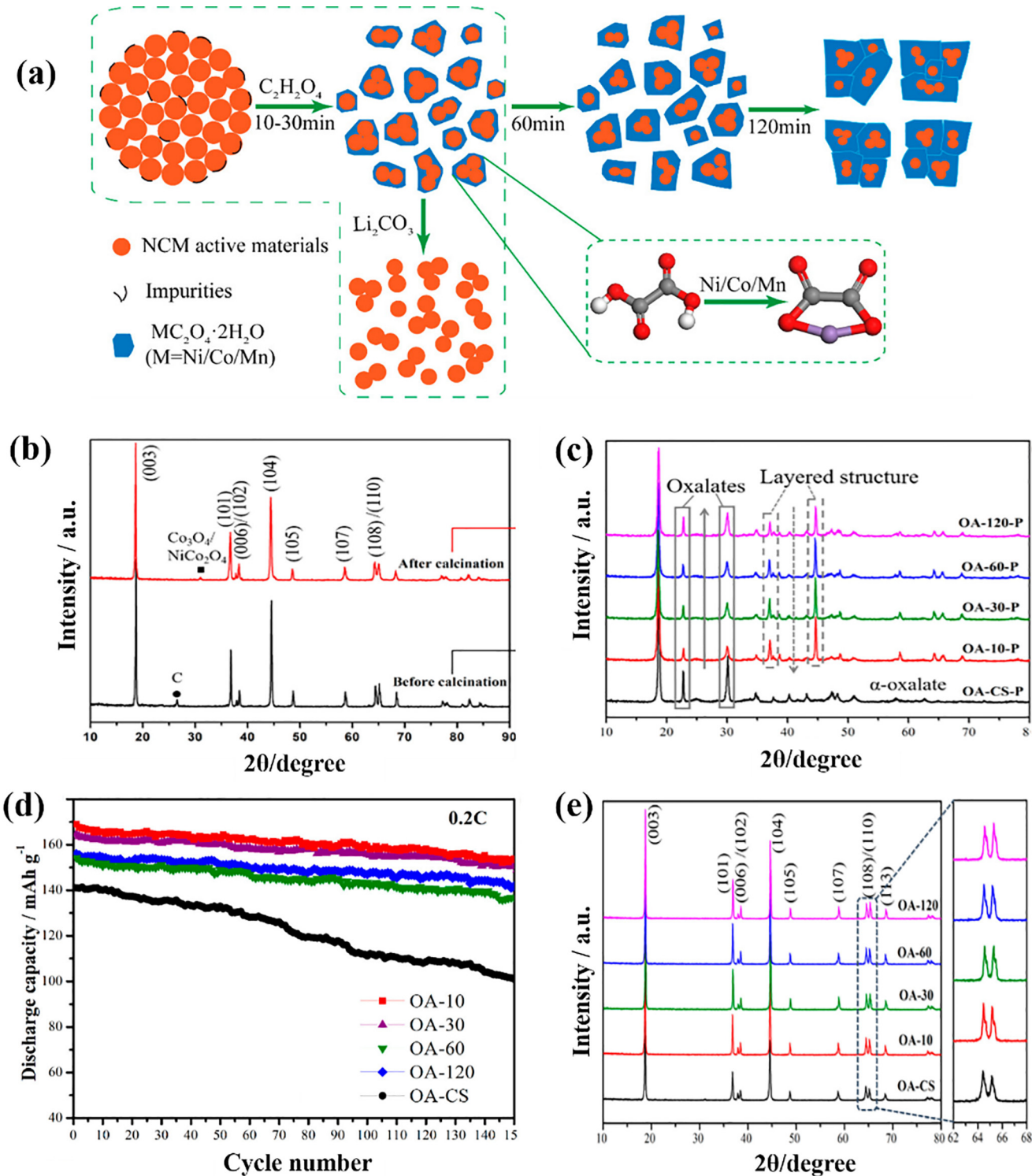


Fig. 14. (a) Illustration of the regeneration process of spent LNCM materials with oxalic acid leaching; (b) XRD patterns of spent LNCM cathodes before and after calcination; (c) XRD patterns of leaching residues with different leaching time and contrast sample; (d) cycling performances of regenerated LNCM cathodes at 0.2 C; (e) XRD patterns of regenerated LNCM cathodes [94].

cycles at 5 C. In another report, $FePO_4 \cdot 2H_2O$ and Li_2CO_3 , which were both recycled from the spent LIBs, were mixed and annealed with sucrose to prepare $LiFePO_4/C$ (Fig. 18), which possessed a discharge capacity of 152.2 and 150.1 mAh g^{-1} under 0.2 and 0.5 C, respectively, closely comparable to the commercial materials [55].

Hydrothermal treatment is another frequently used way to regenerate cathode from the leachate. Wang et al. regenerated $LiFePO_4$ cathode materials from the recovered Li_3PO_4 as Li and P

precursors and commercial $FeSO_4 \cdot 7H_2O$ as Fe precursor via the hydrothermal method [59]. The reason for using Li_3PO_4 rather than Li_2CO_3 , which is the most common form of recycled lithium salt, is that Li_3PO_4 has a smaller solubility than Li_2CO_3 , and as a result, more Li in the leachate can be recovered in the form of Li_3PO_4 . Under the hydrothermal reaction temperature of 200 °C, the recovered $LiFePO_4$ showed a fairly good performance with a discharge capacity of 157.2 mAh g^{-1} at 0.2 C. Moreover, it was also found that

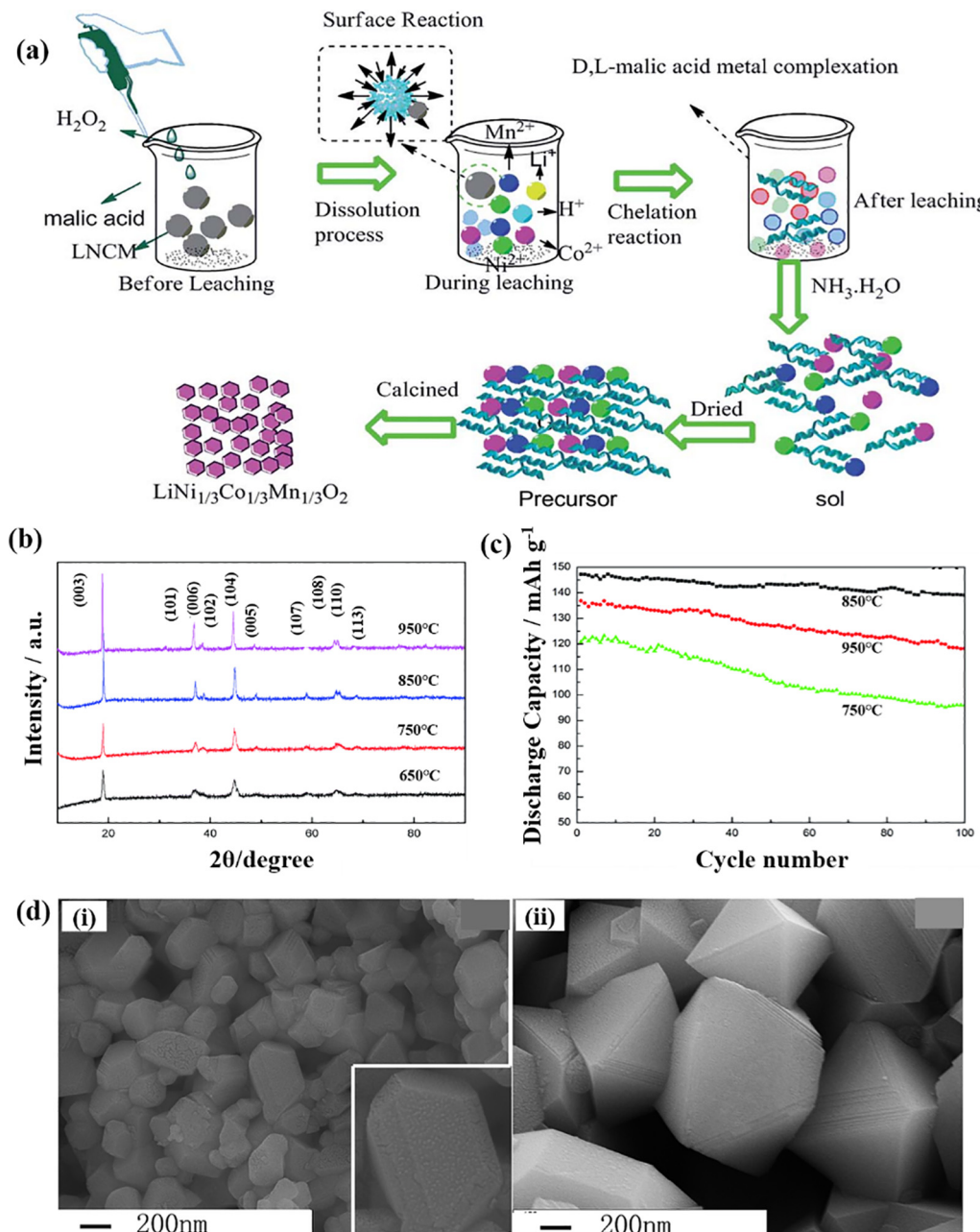


Fig. 15. (a) The scheme of sol-gel regeneration process; (b) XRD patterns of the resynthesized LNCM calcined at different temperatures; (c) the cycling performance of LNCM synthesized at different calcination temperatures; (d) FESEM image of the resynthesized LNCM of (i) edge-blunted polyhedral structure calcined at 850 °C for 6 h in air, (ii) octahedral structure calcined at 950 °C for 6 h in air [99].

the hydrothermal method has distinct advantages over traditional solid-state reaction, in terms of the more controllable particle size, which is favorable for optimizing the intercalation/deintercalation of Li ions. A high reaction temperature leads to a lower growth rate of LiFePO₄ nucleus and smaller LiFePO₄ grains, which can shorten the Li ion diffusion distance and improve the electrochemical performance of the LiFePO₄.

2.3. Direct regeneration of cathode materials

Recently, there has been an ever-growing interest in the direct regeneration of the spent cathode materials. Heat-treatment, solid-state sintering, and hydrothermal method in the presence of Li source are usually used to recover the spent cathode materials. In the solid-state sintering and hydrothermal process, the lost Li

ions in the spent cathode material can be replenished through a relithiation process and the residual PVDF binder can be decomposed during the heat-treatment, which is beneficial in terms of avoiding the particle agglomeration and enhancing electrochemical performance of the obtained material [53,136,137]. Moreover, the impurities and cracks on the spent materials will also be removed and the deteriorated structures, like the spinel and rock salt phases in LiNi_xCo_yMn_zO₂, can be converted back to the desirable layered structure as well [33–35,138,139].

Chen et al. developed a small-scale heat-treatment prototype line to recycle the spent soft package LiFePO₄ batteries (Fig. 19) [136]. The remaining PVDF in the spent LiFePO₄ would cause agglomeration and low tap densities of the untreated spent cathode particles. Under the heat-treatment temperature at 650 °C, the PVDF decomposed and new LiFePO₄ was formed from the

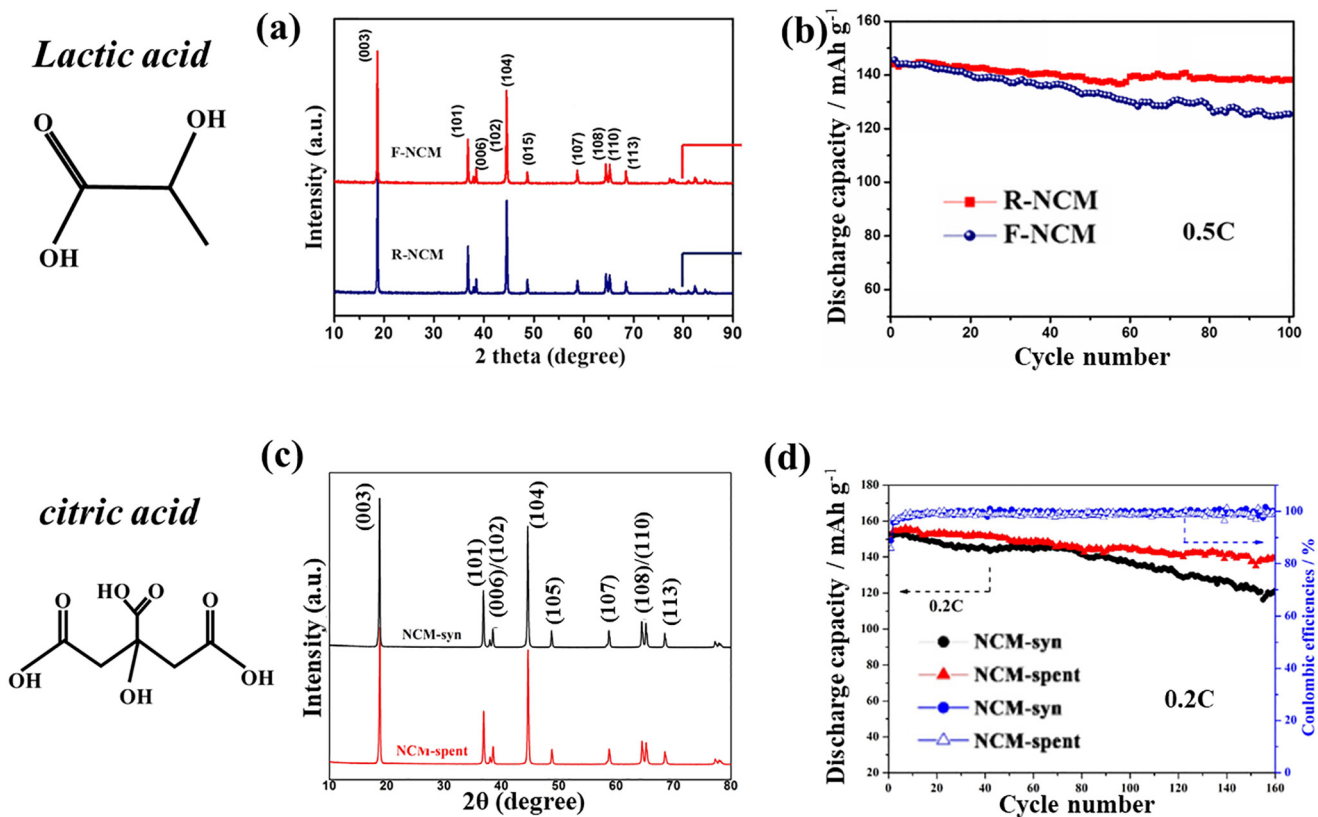


Fig. 16. (a) XRD patterns and (b) the cycling performance of the resynthesized LNCM using lactic acid [63]; (c) XRD patterns and (d) the cycling performance of the resynthesized LNCM using citric acid [61].

Table 4

Summary of the regeneration approaches of LNCM from the spent LIBs.

Regenerated materials	Precursors	Leaching reagents	Precipitant	Initial discharge capacitance/(mAh g⁻¹)	Ref.
$\text{LiNi}_{1/3}\text{Mn}_{1/3}\text{Co}_{1/3}\text{O}_2$	$\text{Ni}_{1/3}\text{Mn}_{1/3}\text{Co}_{1/3}(\text{OH})_2$	H_2SO_4 and H_2O_2	NaOH and $\text{NH}_3\text{-H}_2\text{O}$	152.3 (0.2 C)	[124]
$\text{LiNi}_{1/3}\text{Mn}_{1/3}\text{Co}_{1/3}\text{O}_2$	Oxalate precipitates	Oxalic acid	Oxalic acid	168 (0.2 C)	[94]
$\text{LiNi}_{0.5}\text{Co}_{0.2}\text{Mn}_{0.3}\text{O}_2$	$\text{Ni}_{0.5}\text{Co}_{0.2}\text{Mn}_{0.3}(\text{OH})_2$	Sulfuric acid	NaOH and $\text{NH}_3\text{-H}_2\text{O}$	172.9 (0.2 C)	[109]
$\text{LiNi}_{1/3}\text{Mn}_{1/3}\text{Co}_{1/3}\text{O}_2$	Sol-gel	Maleic acid and H_2O_2	/	151.6 (0.2 C)	[92]
$\text{LiNi}_{1/3}\text{Mn}_{1/3}\text{Co}_{1/3}\text{O}_2$	Sol-gel	Acetic acid and H_2O_2	/	115 (0.2 C)	
$\text{LiNi}_{1/3}\text{Mn}_{1/3}\text{Co}_{1/3}\text{O}_2$	Sol-gel	Citric acid and H_2O_2	/	152.8 (0.2 C)	[61]
$\text{LiNi}_{1/3}\text{Mn}_{1/3}\text{Co}_{1/3}\text{O}_2$	$\text{Ni}_{1/3}\text{Co}_{1/3}\text{Mn}_{1/3}\text{CO}_3$	H_2SO_4 and H_2O_2	Na_2CO_3 and $\text{NH}_3\text{-H}_2\text{O}$	163.5 (0.1 C)	[127]
$\text{LiNi}_{1/3}\text{Mn}_{1/3}\text{Co}_{1/3}\text{O}_2$	$\text{Ni}_{1/3}\text{Mn}_{1/3}\text{Co}_{1/3}(\text{OH})_2$	H_2SO_4 and H_2O_2	NaOH and $\text{NH}_3\text{-H}_2\text{O}$	150.6 (0.1 C)	[128]
$\text{LiCo}_{0.415}\text{Mn}_{0.435}\text{Ni}_{0.15}\text{O}_2$	$\text{Co}_{0.415}\text{Mn}_{0.435}\text{Ni}_{0.15}\text{O}_2(\text{OH})_2$	HNO_3 and H_2O_2	NaOH	64.7	[123]
$\text{LiNi}_{1/3}\text{Mn}_{1/3}\text{Co}_{1/3}\text{O}_2$	/	HNO_3 and urea	/	122.21	[129]
$\text{LiNi}_{1/3}\text{Mn}_{1/3}\text{Co}_{1/3}\text{O}_2$	Sol-gel	Lactic acid and H_2O_2	/	151.6 (0.2 C)	[63]
$\text{LiNi}_{1/3}\text{Mn}_{1/3}\text{Co}_{1/3}\text{O}_2$	Sol-gel	D, L-malic acid and H_2O_2	/	147.2 (0.2 C)	[99]
$\text{LiNi}_{0.8}\text{Co}_{0.1}\text{Mn}_{0.1}\text{O}_2$	$\text{Ni}_{0.8}\text{Co}_{0.1}\text{Mn}_{0.1}(\text{OH})_2$	H_2SO_4 and H_2O_2	NaOH and $\text{NH}_3\text{-H}_2\text{O}$	197.7 (0.1 C)	[130]
$\text{LiNi}_{0.5}\text{Co}_{0.2}\text{Mn}_{0.3}\text{O}_2$	$\text{Ni}_{0.5}\text{Co}_{0.2}\text{Mn}_{0.3}(\text{OH})_2$	H_2SO_4 and H_2O_2	NaOH and $\text{NH}_3\text{-H}_2\text{O}$	174.3 (0.1 C)	
$\text{LiNi}_{1/3}\text{Mn}_{1/3}\text{Co}_{1/3}\text{O}_2$	$\text{Ni}_{1/3}\text{Mn}_{1/3}\text{Co}_{1/3}(\text{OH})_2$	H_2SO_4 and H_2O_2	NaOH and $\text{NH}_3\text{-H}_2\text{O}$	168.3 (0.1 C)	
$\text{LiNi}_{1/3}\text{Mn}_{1/3}\text{Co}_{1/3}\text{O}_2$	$\text{Ni}_{1/3}\text{Mn}_{1/3}\text{Co}_{1/3}(\text{OH})_2$	H_2SO_4 and H_2O_2	NaOH and $\text{NH}_3\text{-H}_2\text{O}$	155 (0.1 C)	[131]
$\text{LiNi}_{1/3}\text{Mn}_{1/3}\text{Co}_{1/3}\text{O}_2$	$\text{Ni}_{1/3}\text{Mn}_{1/3}\text{Co}_{1/3}(\text{OH})_2$	Citric acid and H_2O_2	Ammonia solution	154.2 (0.2 C)	[48]
$\text{LiNi}_{1/3}\text{Mn}_{1/3}\text{Co}_{1/3}\text{O}_2$	$\text{Ni}_{1/3}\text{Mn}_{1/3}\text{Co}_{1/3}(\text{OH})_2$	H_2SO_4 and H_2O_2	NaOH and $\text{NH}_3\text{-H}_2\text{O}$	158 (0.1 C)	[132]
$\text{Li}_{1.2}\text{Co}_{0.13}\text{Ni}_{0.13}\text{Mn}_{0.54}\text{O}_2$	/	Ascorbic acid	Oxalic acid	258.8	[133]
$\text{LiNi}_{1/3}\text{Mn}_{1/3}\text{Co}_{1/3}\text{O}_2$	$\text{Ni}_{1/3}\text{Mn}_{1/3}\text{Co}_{1/3}(\text{OH})_2$	H_2SO_4 and H_2O_2	NaOH	/	[134]
$\text{LiNi}_{1/3}\text{Mn}_{1/3}\text{Co}_{1/3}\text{O}_2$	$\text{Ni}_{1/3}\text{Mn}_{1/3}\text{Co}_{1/3}(\text{OH})_2$	H_2SO_4 and H_2O_2	NaOH	160	[135]
$\text{Li}[(\text{Ni}_{1/3}\text{Co}_{1/3}\text{Mn}_{1/3})_{1-x}\text{Mg}_x]\text{O}_2$	/	H_2SO_4 and H_2O_2	/	152.7 (0.2 C)	[46]

FePO_4 , Fe_2O_3 , P_2O_5 and Li_3PO_4 that were derived from the decomposed LiFePO_4 materials during previous battery cycles. The recovered cathode materials showed the same discharge capacity as the pristine ones. This work thus provides the possibility for the industrial-scale heat-treatment method.

In spite of the progress, the problem of Li ion deficiency can not be solved in the direct heat-treatment process and the regenerated cathode's long-term performance can't be guaranteed. To solve this issue, Li et al. regenerated LiFePO_4 by co-sintering the spent cath-

odes with Li_2CO_3 and the recovered LiFePO_4 material possessed a fairly high specific discharge capacity of 140.4 mAh g^{-1} at 0.2 C [138]. Another simple direct regeneration process by solid-state sintering was proposed by Song et al. [36]. By sintering the pristine LiFePO_4 together with the spent ones, a high specific capacity of 144 mAh g^{-1} was obtained, with a ratio of 3:7 of the two materials and at a heating temperature of 700°C . The performances of the as-obtained LiFePO_4 cathode material can meet the basic requirements for reuse.

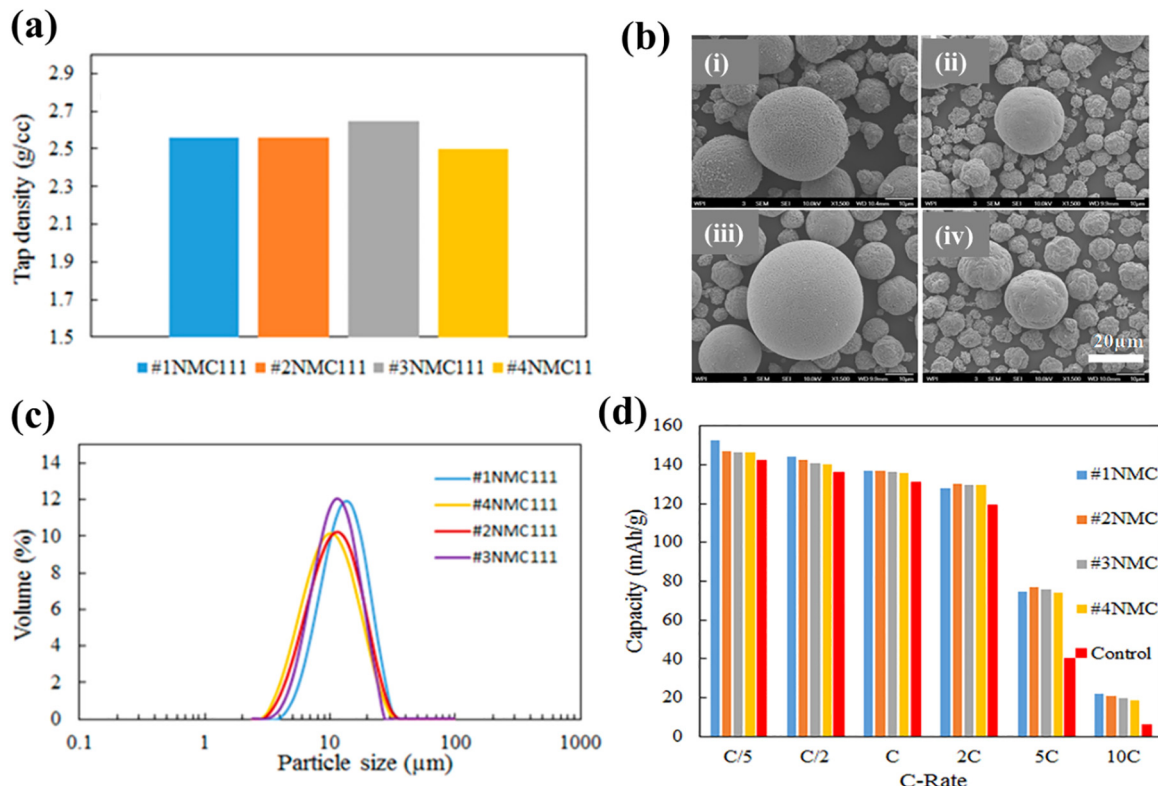


Fig. 17. (a) The tap density for the cathode materials from the four different recycling streams: #1NMC111 (NMC + LMO), #2NMC111 (NMC + LMO + LFP), #3NMC111 (NMC + NCA + LMO), #4NMC (NMC + NCA + LMO + LCO + LFP); (b) SEM images of (i) #1NMC111, (ii) #2NMC111, (iii) #3NMC111, (iv) #4NMC; (c) particle size distribution of the four cathodes; (d) rate performance of the four cathodes [124].

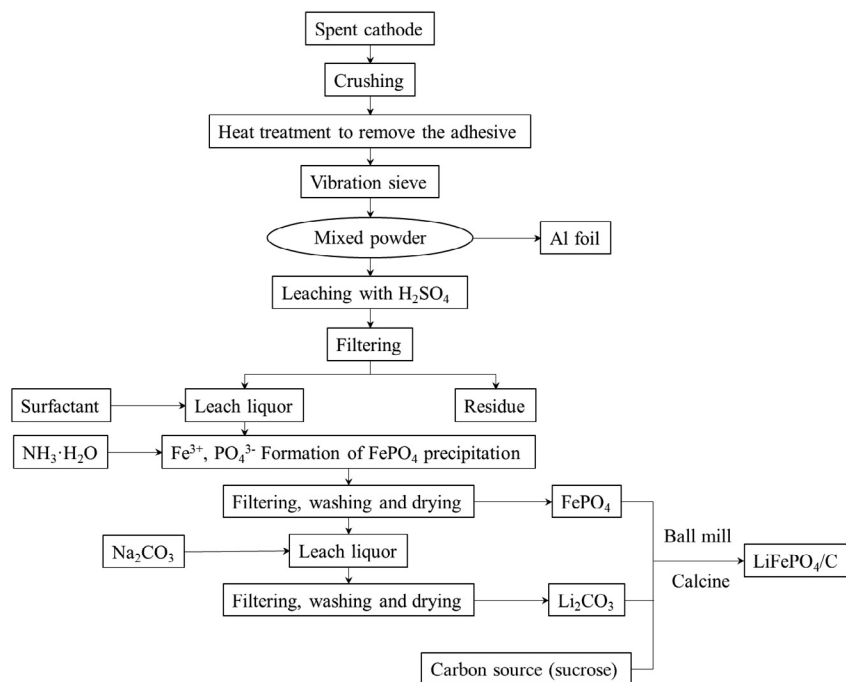


Fig. 18. Flowsheet for the spent LiFePO₄ cathode recycling process via carbon thermal reduction method [55].

Similar to the LiFePO₄ materials, Zhou et al. also found that impurities such as LiF, Li₂CO₃, and LiMn₂O₄ existed on the surface of the spent LiNi_{0.5}Co_{0.3}Mn_{0.2}O₂ cathodes [33]. On this basis, the spent LiNi_{0.5}Co_{0.2}Mn_{0.3}O₂ material was mixed with lithium acetate and annealed together to replenish Li into the material lattice and

remove the impurities and cracks. In addition, it was also found that the spinel and rock salt structure were also removed during the process. The regenerated material showed an excellent electrochemical performance with a discharge capacity of 164.6 mAh g⁻¹ at 0.1 C and 147 mAh g⁻¹ at 1 C, respectively. Moreover, high capacity

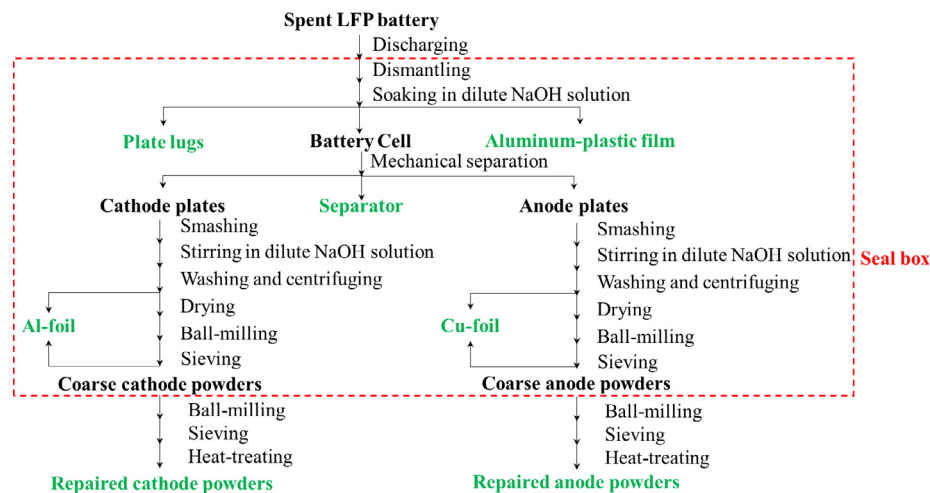


Fig. 19. The recycling process flow diagram of the soft package spent LiFePO₄ battery [136].

retention of 89.12% was obtained after 100 cycles at 1 C. In another study, Li et al. annealed the spent LiNi_{0.5}Co_{0.2}Mn_{0.3}O₂ with LiOH-H₂O to regenerate LiNi_{0.5}Co_{0.2}Mn_{0.3}O₂ cathode materials [35]. The recovered cathode possessed reconstructed structure and low level of cation mixing, which is beneficial for the transfer of Li ions.

As above-mentioned, the MC method can facilitate the direct regeneration of the spent cathode materials. Meng et al. incorporated the MC activation process with the solid-state annealing to regenerate the LiNi_{1/3}Co_{1/3}Mn_{1/3}O₂ cathode materials [140]. The MC activation helped to decrease the particle size and reduce the length of ion diffusion to improve the reversibility of the Li ions intercalation/deintercalation, which is beneficial for alleviating the cation mixing and promoting the reconstruction of the layered structure. The regenerated cathode material had an initial discharge capacity of 165 mAh g⁻¹ at 0.2 C and capacity retention of above 80% after 100 cycles, which was even better than the pristine LiNi_{1/3}Co_{1/3}Mn_{1/3}O₂ synthesized by a single solid-state method. Xu et al. developed a strategy to regenerate LiFePO₄ via MC-assisted solid-state technique and V⁵⁺ doping [141]. In this process, the MC treatment can ensure the reduction of the crystallinity, uniform mixing of the precursors, and nanocrystallization of the raw materials; while doping the material with V⁵⁺ helps improve the electrochemical performance with a discharge capacity of 154.3 mAh g⁻¹ at a rate of 0.1 C. Due to this, MC methods have great potential in both hydrometallurgy recycling and direct regeneration of the spent LIBs.

Different from direct solid-state synthesis, in the process of the hydrothermal method, the calculation to adjust the Li/Fe ratio may not be compulsory because Li is not easy to volatilize during the hydrothermal reaction compared to solid-state sintering [34,139]. Shi et al. proposed a two-step approach to directly regenerate the degraded LiNi_{1/3}Co_{1/3}Mn_{1/3}O₂ and LiNi_{0.5}Co_{0.2}Mn_{0.3}O₂ cathode materials [34]. By combining the hydrothermal treatment with a subsequent annealing process, Li ions were replenished to the Li vacancy and the spinel/rock salt phase was converted back to the layered structure (Fig. 20a, b). The regenerated particles remained their original morphology and exhibited a high specific capacity, good cycling stability, and high rate performance that are equal to the pristine materials (Fig. 20d-g). In this study, the effect of nickel content and oxygen partial pressure on the direct solid-state sintering regeneration process was investigated. It was found that cation mixing is more serious in the Ni-rich cathode materials and a higher O₂ partial pressure is needed to eliminate the rock salt phase on the surface of LiNi_{0.5}Co_{0.2}Mn_{0.3}O₂ cathode.

Song et al. also utilized the hydrothermal method to regenerate LiFePO₄ through Li-ion compensation and repair of the destructive crystal [139]. Meanwhile, before the hydrothermal process at a temperature of 160 °C for 6 h, graphene oxide, which was obtained from the spent anode graphite through typical Hummer's method, was added to form LiFePO₄/graphene composite during the hydrothermal reaction. The LiFePO₄ particles distributed in the interlayer space of graphene (Fig. 20h, i), which could improve the electronic conductivity of the regenerated LiFePO₄. In comparison with the materials regenerated by solid-state sintering at 650 °C for 2 h (C-650-2), the hydrothermally fabricated composite with 5% graphene showed a higher capacity and more stable cycling performances (Fig. 20j, k).

The direct regeneration process, as a measurement to repair the spent cathode materials, doesn't need to destroy the crystal structure of the cathode. As a simple low-cost and energy-efficient recycling route, this acid-free process is environmentally friendly with little secondary pollution compared with the hydrometallurgy method. Besides, direct regeneration may be applicable to low-value spent cathodes (e.g., LFP and LMO) which are not profitable when adopting pyrometallurgy or hydrometallurgy method. Based on these characteristics, it is regarded as an economically competitive and promising recycling method in the future. However, the properties of the recovered cathode materials depend heavily on the quality of the spent batteries and even a small amount of impurity (e.g., Al) can significantly deteriorate the material's electrochemical performance. Therefore, process parameters need to be very carefully adjusted to ensure the high purity of the regenerated cathode. In this case, one certain direct regeneration method cannot accommodate all sorts of spent cathodes when the best product quality is considered. Mixed types of feedstocks in the practical recycling process may pose serious challenges for the application of this method [142].

3. Recycling of graphite anodes

With the wide deployment of LIBs in EVs or grid-scale energy storage facilities, the demand of graphite to synthesize anode will increase greatly. In the spent LIBs, there is about 12 wt%–21 wt% of graphite, which is quite a considerable amount. The countries that do not produce graphite or have a low reserve of it, like the United States and European Union countries, regard flake graphite as a critical material [143,144]. Moreover, recycled graphite can also

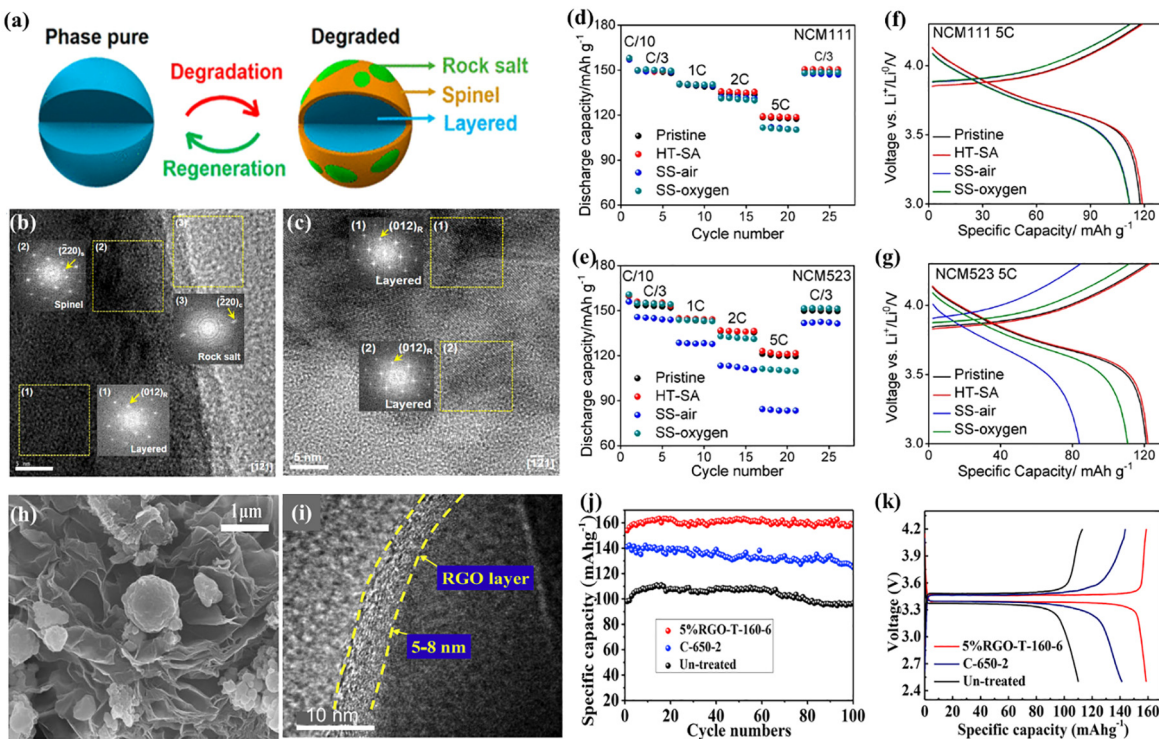


Fig. 20. (a) Illustration of the crystal structure change of $\text{LiNi}_{0.5}\text{Co}_{0.2}\text{Mn}_{0.3}\text{O}_2$ after cycling and regeneration; (b, c) HRTEM image and FFT images of cycled/degraded $\text{LiNi}_{0.5}\text{Co}_{0.2}\text{Mn}_{0.3}\text{O}_2$ particles and $\text{LiNi}_{0.5}\text{Co}_{0.2}\text{Mn}_{0.3}\text{O}_2$ particles after hydrothermal and annealing treatment, respectively; (d, e) rate performance of NCM111 and NCM523 samples, respectively; (f, g) charge-discharge profiles of NCM111 and NCM523 samples at 5 C, respectively [34]; (h) SEM image and (i) HRTEM image of the LiFePO_4 /graphene sample; (j) cycle performances and (k) charge-discharge profiles of a full battery using regenerated LiFePO_4 at 0.2 C [139].

be a very desirable raw material for the preparation of other functional materials. Therefore, the re-utilization of the graphite anode has great strategic importance and practical feasibility.

3.1. Regenerating graphite and recycling lithium

It has been reported that the spent anode graphite can be reused as high capacity anode in new batteries after regeneration [145]. Moreover, the content of lithium in the anode of spent LIBs is much higher than the environmental abundance [39]. As a result, the recycling of anode can recover both the valuable Li element and graphite. For instance, Yang et al. proposed a process to simultaneously recycle lithium and regenerate graphite, as shown in Fig. 21(a) [146]. This two-step thermal treatment method can separate the graphite from copper foil and oxidize the remaining copper element in graphite to make it easily removed by acid. After leaching by HCl, pure graphite was obtained with Li, Al, and Cu remaining in the leachate. After adjusting the pH to remove Al^{3+} and Cu^{2+} , Li was recovered in the form of Li_2CO_3 after adding Na_2CO_3 into the solution. The regenerated graphite showed a high initial discharge capacity of 591 mAh g^{-1} at 37.2 mA g^{-1} and 97.9% of capacity retention after 100 cycles. The high lithium storage capacity was in accordance with its expanded interlayer spacing and smaller particles.

Besides, many researchers have been committed to recovering the spent anode graphite to further prepare functional materials, such as the cathodes for the electro-Fenton system [147], polymer-graphite nanocomposites [148], and MnO_2 -modified graphite sorbents [37]. For instance, Cao et al. have recycled anode scrap and used the reclaimed graphite as the cathode in the electro-Fenton system for pollutant degradation [147]. The acid-leaching treated graphite achieved 100% bisphenol A (BPA) removal in 70 min and 87.4% chemical oxygen demand (COD)

removal in 240 min. Moreover, using the spent graphite as the raw material, Zhao et al. prepared MnO_2 -modified artificial graphite (MnO_2 -AG) sorbents to treat contaminated water [37]. After the heat-treatment of the spent anode, the surface of the graphite was decorated by MnO_2 particles by immersing the graphite in a KMnO_4 solution. The MnO_2 -AG showed 99.9%, 79.7%, and 99.8% removal efficiencies towards Pb (II), Cd (II), and Ag (I), respectively, which were much better than the pristine AG (Fig. 21b, c).

3.2. Synthesis of graphene from spent anode graphite

Graphene, a single-atom-thick monolayer sheet of carbon atoms, has appealed a lot of research interests since it was found in 2004 [149]. It has been considered as one of the most promising materials for various applications owing to its outstanding properties like high thermal and electrical conductivity and strong mechanical strength [150,151]. Up to now, the raw materials used for graphene fabrication are usually natural graphite, which is difficult to exfoliate. In contrast, the interplanar spacing of the anode graphite material increases during the repeated charge/discharge process, resulting in a weakened Van der Waals' force between the graphitic layers [152]. This makes the graphite easier to be exfoliated to graphene and the attached oxygen-contained groups can prevent it from aggregation.

In a typical example, Zhang et al. reused the spent anode graphite to prepare graphene [153]. It was found that the spent graphite maintained a layered structure and consisted of oxygen groups in the interlayer spacing, which is beneficial for the oxidation reaction. Graphite oxide was obtained by Hummers' method using the spent graphite as the raw material, and graphene was obtained after a subsequent ultrasonic exfoliation and reduction process. Compared to the "natural graphite \rightarrow graphene" process, the consumption of H_2SO_4 and KMnO_4 decreased by 40% and

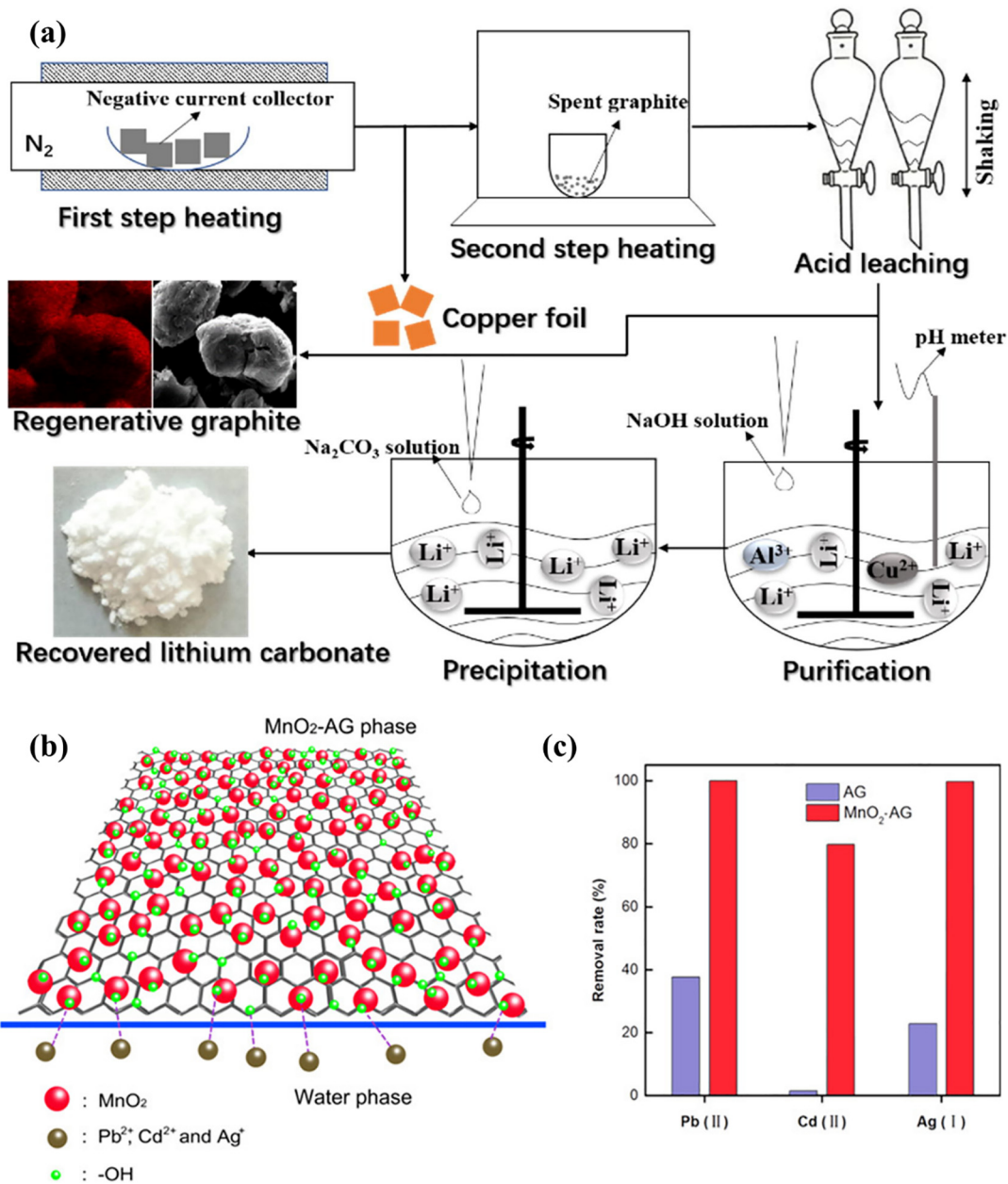


Fig. 21. (a) Flow chart of the whole recycling process of anode [146]; (b) schematic diagram of MnO₂-AG and (c) comparison of removal rates of Pb(II), Cd(II), and Ag(I) between MnO₂-AG and AG [37].

28.6%, respectively, in this method, due to the presence of oxygen groups and structural defects in the spent graphite material.

However, the large amount of the toxic N₂H₄·H₂O reducing agent required in the reduction process can be another problem. Thus, it is necessary to develop more environmentally friendly reductants. With this purpose, Natarajan et al. prepared rGO using the packaging materials (i.e., Al and stainless steel) from the spent LIBs as the reductant in the presence of HCl and investigated the as-obtained graphene's application in supercapacitor [38]. Among the rGOs synthesized by different reductants at different temperatures, the room-temperature Al-reduced graphene oxide showed the highest specific capacitance of 112 F g⁻¹ at 0.5 A g⁻¹, which is attributed to its high surface area and mesoporous nature. In another study, they synthesized Al-reduced rGO from anode graphite and carbon hollow spheres (CHS) from the separator and studied their gas storage ability [154]. Both CHS and rGO exhibited

efficient gas storage capacities for CO₂. The CO₂ uptake was 12 wt% and 33 wt% for rGO and CHS, respectively, at 40 bar and 298 K. These studies achieved the comprehensive reutilization of the spent LIBs and reduced the consumption of poisonous reductants.

Although the oxidation-reduction method is highly efficient, it could severely destroy the crystal structure of graphene, resulting in poor performance. Besides, the consumption of a large number of additional chemicals also increases the cost. Alternatively, many researchers have been devoted to preparing graphene using anode graphite through "non-chemistry" methods. For example, Chen et al. used the spent graphite to prepare graphene by the sonication aided liquid-phase exfoliation method in an aqueous surfactant solution of sodium cholate [40]. The obtained graphene was less than 4 layers and the exfoliation efficiency of the spent graphite was 3 to 11 times higher than that of natural graphite, due to the reduced interlayer force of the spent graphite. A high electri-

cal conductivity up to 9100 S m^{-1} was achieved on the as-obtained graphene, because of their high quality. In another study, Zhang et al. combined H_2SO_4 leaching and shear mixing to prepare graphene from the used graphite. It was found that the production efficiency was 10 times higher than using the pristine graphite powders and the obtained graphene exhibited excellent stability in an aqueous suspension (Fig. 22a, b) [152]. In this process, the acid treatment didn't destroy the crystal structure but further swelled the graphite lattice (Fig. 22c, d). In addition, they also tested the mechanical performance of the graphene/epoxy composite and found that it exhibited enhanced flexural strength, elastic modulus, and toughness resulted from the functional groups on the graphene sheets that can prohibit the aggregation of graphene sheets and lead to stronger bonding strength between graphene and epoxy (Fig. 22e).

To sum up, as an important strategic resource and promising candidate for graphene preparation, more attention should be paid to the recycling of the spent anode graphite of LIBs.

4. Discussion

The LIBs using the Ni-rich type cathodes, such as NCM523, NCM622, and NCM811, are highly promising for energy-intensive applications and will come in large quantities in the market of new energy vehicles in the next few years. Therefore, feasible recycling strategies, which are indiscriminate to different compositions and practicable for regenerating Ni-rich LNCMs if possible, need to be developed with the highest priority to treat the spent Ni-rich LNCM.

For the leaching process during the hydrometallurgical method, the leaching of Ni-rich cathode materials can be achieved more easily with a shorter time and higher leaching efficiency than ordinary NCM111 types. The increased leaching efficiency of Ni^{2+} , Co^{2+} , and Mn^{2+} can be attributed to the decreased particle size and the phase transformation of Ni-rich cathode [155]. The decreased par-

ticle size increases the specific surface area with more reaction sites for leaching. The phase transformation from layered structure to spinel and rock salt structures is caused by severe cation mixing of Ni-rich cathode. Therefore, the crystal structures of the Ni-rich types are unstable and tend to be destroyed by leaching agents. Compared with transition metal special, a lower leaching efficiency for Li-ions exist for the Ni-rich LNCM materials, because such cathode materials tend to react with air and form LiOH and Li_2CO_3 , which are difficult to be dissolved and will reside on the surface of the particles. Nevertheless, the Ni-rich types still present great feasibility for recycling, and a more insightful understanding of the leaching kinetics is required, and therefore it definitely calls for more detailed research on the leaching process and the corresponding mechanism.

As for the regeneration process in the hydrometallurgical method, the electrochemical performance of the regenerated cathode materials is closely related to the precursors' morphology, crystal structure, and stability. Compared with the regenerated precursors (e.g., $\text{Ni}_{1/3}\text{Co}_{1/3}\text{Mn}_{1/3}\text{CO}_3$) in the carbonate or oxalate form, those regenerated in a hydroxide form (e.g., $\text{Ni}_{1/3}\text{Mn}_{1/3}\text{Co}_{1/3}(-\text{OH})_2$) are more favorable as a precursor to fabricate new LNCM cathode materials, due to their spherical shape and high tap density. Though obtaining spherical shape and uniform dispersion, most of the resynthesized LNCM are secondary agglomerates, which may pose problems like structural deterioration when recycled in high-voltage situations. The single-crystal structure, on the other hand, shows good stability in cycling performance and has stimulated great interests of industrial-scale manufacturing in some companies. Thus, it is reasonable for more attention to be paid on the recycling of spent LIBs to prepare the single-crystal structure.

The co-precipitation method is also applicable in recycling and regenerating Ni-rich LNCM. The regeneration of Ni-rich LNCM through the hydroxide co-precipitation method achieves satisfactory initial discharge capacitance of 197.7 mAh g^{-1} for $\text{LiNi}_{0.8}\text{Co}_{0.1}-\text{Mn}_{0.1}\text{O}_2$ and 174.3 mAh g^{-1} for $\text{LiNi}_{0.5}\text{Co}_{0.2}\text{Mn}_{0.3}\text{O}_2$ [124]. Even though, the as-prepared Ni-rich materials still face the problem

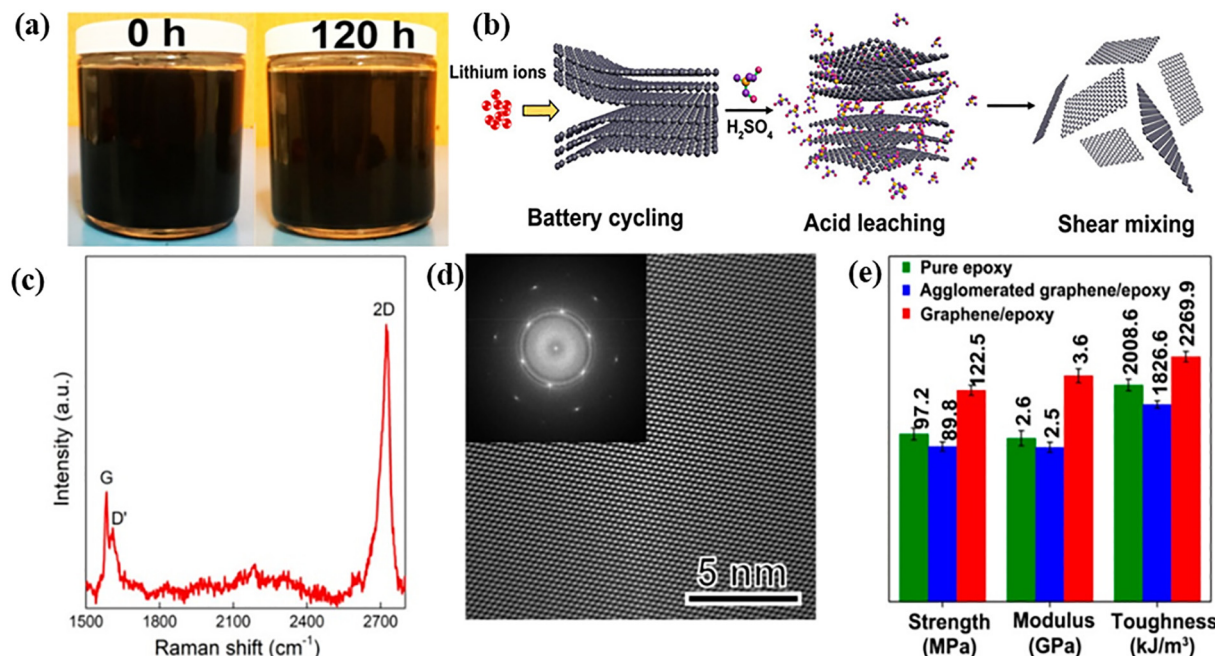


Fig. 22. Fabrication of graphene from acid-treated anode graphite. (a) Chronological digital photos of graphene suspension derived from acid-treated anode graphite; (b) schematic diagram of the graphite lattice expansion due to battery cycling and acid leaching; (c) Raman spectrum of the as-fabricated graphene; (d) convoluted lattice image of graphene sheet derived from acid-treated anode graphite, showing no visible defects; and (e) comparison of flexural strength, elastic modulus, and toughness for pure epoxy and composites reinforced by agglomerated graphene derived from pristine graphite and graphene from acid-treated anode graphite [152].

of poor cycling performance, which is the inherent characteristic of Ni-rich types and researchers have paid great efforts to improve cycling performance by optimizing the preparation process. Therefore, it is possible that those strategies used for enhancing the stability of Ni-rich LNCM materials can also be feasible to be adopted in their hydrometallurgical regeneration process, such as metal doping, surface coating, or increasing the valence state of Ni [156–158].

Apart from the hydrometallurgical regeneration, LNCM can also be regenerated by the direct regeneration method, which is, however, more difficult compared with the regeneration of other types of cathode materials because of the cation mixing in it, especially for the Ni-rich materials [159]. For example, it was found that LNCM needs a higher hydrothermal regeneration temperature than LiCoO₂, due to the Li⁺/Ni²⁺ mixing that causes a higher activation energy barrier for the diffusion of Li ions [34]. Besides, with the continuously increased Ni content in the LNCM nowadays, the cation mixing issue becomes more serious, and direct regeneration of such material becomes more difficult as well.

As for LFP, the hydrometallurgical recycling route has a relatively lower economic viability, which is attributed to the low value of the LFP material and the consumption of chemical reagents during its regeneration. For this reason, alternative low-cost and acid-free direct regeneration methods have been considered more feasible for recycling the LFP batteries, now and in the future. For example, Li et al. developed a simple and low-cost direct regeneration process for spent LFP batteries by ball-milling spent LFP with Li₂CO₃, and they were further directly sintered at 700 °C for 3 h. The regenerated LFP cathode possessed a high discharge capacity of 151.55 mAh g⁻¹ and capacity retention of 97.77% after 200 cycles at 0.2 C [160]. Interestingly, E. Shangguan et al. regenerated LiFePO₄ by the direct regeneration method and used it as the anode for alkaline Ni-Fe secondary batteries [161,162]. With the addition of Bi₂S₃ or FeS, the LiFePO₄/Bi₂S₃ and LiFePO₄/C/FeS composites showed excellent anodic performance, and this study demonstrated a facile way to recycle the spent LFP materials and offered an attractive candidate anode material for alkaline Ni-Fe batteries as well, which sheds light on further improving the economic benefits of LFP batteries.

Except for the exhausted LIBs, there is a large amount of electrode scraps produced from both research and industrial activities, which have not undergone the charge-discharge process and do not have the problems of Li loss or impurities on the particle surface [47,137]. The only negative influence on their recycling is caused by the PVDF binder to result in the agglomeration of the active material particles. Hence, these electrode scraps can be reused if the remnant PVDF can be effectively removed. In this case, the electrode scraps are more suitable to be recycled by the direct heat-treatment method, which has the obvious advantages compared with other recycling methods for its lower cost and simpler operation [163]. For example, Zhang et al. used different pretreatment process, such as thermal treatment, NMP dissolution, and alkaline dissolution, followed by the heat-treatment to regenerate the Li(Ni_{1/3}Co_{1/3}Mn_{1/3})O₂ scraps [137] and the results demonstrated that the recycled cathode material exhibited satisfactory electrochemical performances, with a discharge capacity of 150.2 mAh g⁻¹ at 0.2 C after 100 cycles and a capacity retention of 95.1%. However, the temperature for the heat-treatment should be properly manipulated. A too low temperature cannot remove the PVDF completely; while a too high temperature will cause the release of HF from the decomposed PVDF that will react with the cathode materials, causing the deterioration of the crystal structure and formation of impurities, such as LiF and transition metal oxides.

5. Conclusions and perspective

With the rapid inflating of the market share of electric vehicles and other electronic devices, which are heavily relied on the high energy/power LIBs, the development of appropriate disposal technologies of the spent LIBs becomes increasingly urgent. From the viewpoints of protecting the environment and saving non-renewable resources, recycling the spent LIBs brings numerous benefits.

The pretreatment aims to separate active materials from the current collectors by removing the PVDF binder or Al foil current collector. Some pretreatment methods (e.g., thermal treatment) can cause the change of the valence state of metals, which is helpful for the subsequent leaching and separation of the metal species. However, at the current stage, the volumes of the batteries used in vehicles are usually too large to be dismantled manually. Therefore, it is necessary to develop automatic dismantlement technologies to ensure the safety and efficiency of the pretreatment, which will, in turn, facilitate the industrial-scale battery recycling as well.

The hydrometallurgical method is the most widely adopted method for the recycling of LIBs, because of its high recovery efficiency and low energy consumption. During the leaching process, the shrinking-core model and Avrami equation have been the widely accepted models to exactly describe the leaching process and furthermore direct the researchers to improve the leaching efficiency.

Selective leaching to extract special valuable metal elements has been proven feasible for recycling LFP, which selectively leaches the valuable Li out of Fe and avoids the complex steps to separate metal ions. As for the recycling of LiCoO₂, oxalic acid has been used to retrieve Li and Co in the form of oxalate precipitants. To be forward-looking, if the valuable Co element could be selectively leached with other metal elements remained in the residue, the whole recycling procedure of the LNCM materials will be effectively shortened and the costs will be decreased as well.

In contrast to the traditional inorganic leaching reagents, the organic ones are more promising due to their eco-friendly, biodegradable, and recyclable characteristics. The leaching capability of organic acids towards metal species is attributed to both the acidity of H⁺ and the chelating capability of the anion ions. Furthermore, the gel networks, formed by the chelation of metal ions and organic acids, can be used as the precursors of sol-gel regeneration. Therefore the organic acids leaching always cooperate with sol-gel regeneration. Additionally, the organic acids have other multiple functionalities, such as the precipitating and reducing properties.

Reducing agents can decrease the activation energy of acid dissolving by reducing the valence states of metal ions. Among multiple reducing reagents, H₂O₂ presents excellent properties with low toxicity and eco-friendliness. Except for using the typical H₂O₂ reducing agent, the carbothermal reduction method, whose raw materials are cost-effective, is also practicable to reduce the valence state and change the crystal structure of cathode materials.

MC method is a technology for the effective recycling of valuable metals from the spent LIBs. It can decrease the particle size and increase the reactivity of the cathode materials by introducing an intensified ball-milling process and some chelating reagents, which can facilitate the following leaching process. MC process can also realize the selective leaching of metal ions with the help of some adding agents (e.g., H₂O₂).

The reclaiming of precursors from the leachate for synthesizing new cathode materials generally includes co-precipitation and sol-gel methods. The quality of the precursor determines the final performance of the obtained cathode material. Both the co-precipitation method and the sol-gel method avoid the complex procedures to separate different metal ions by selective precipita-

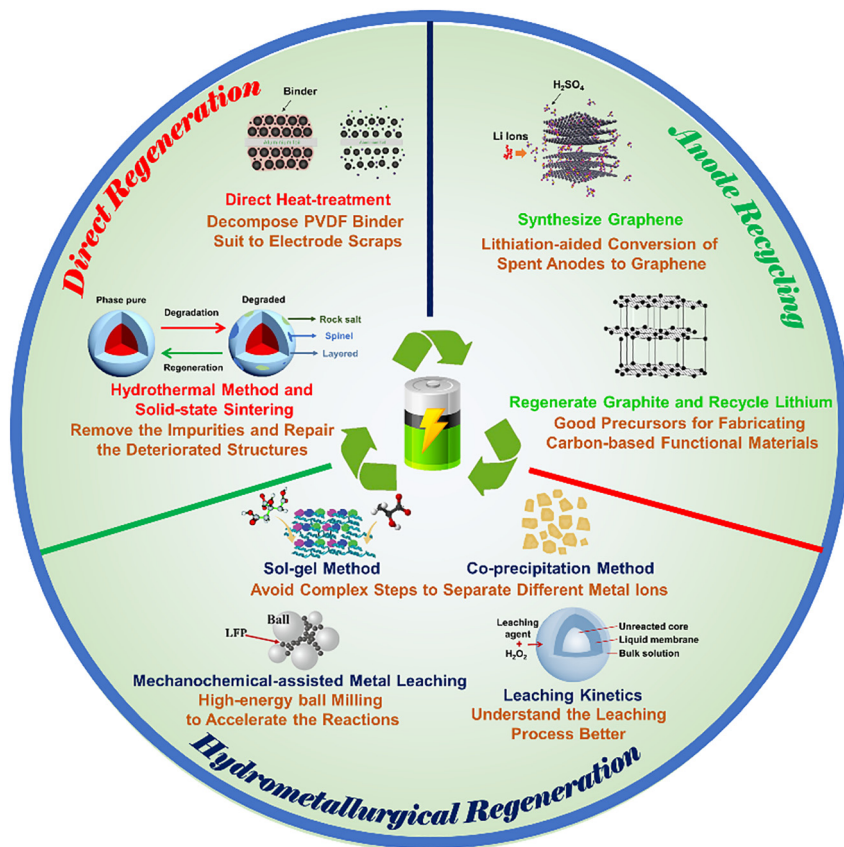


Fig. 23. The summary of the major technologies for recycling the LiFePO_4 and $\text{LiNi}_{1-x}\text{Co}_y\text{Mn}_2\text{O}_4$ cathode materials by hydrometallurgical regeneration and direct regeneration method, and the technologies for recycling graphite anode.

tion and extraction. Meanwhile, they also achieve closed-loop recycling for LIBs with the valuable cathode products obtained.

Compared with the hydrometallurgical method, the direct regeneration of spent cathode materials is simpler and more effective to repair cathode materials and restore its original electrochemical performance. It will greatly reduce the costs if applied in the industry in the future. For the Ni-rich LNCM batteries, which have a high energy density feature and have occupied a large portion of the market of electric vehicles, the direct regeneration of the retired LNCM materials is, however, uneasy because of the serious cation mixing after the repeated charge-discharge cycles. Thus, new technologies for the direct regeneration of the spent Ni-rich batteries should be developed. It is also worth noting that new cathode materials are continuously and rapidly emerging, which requires recycling technologies to keep pace with the development of cathode materials. Besides, considering that the spent batteries from the market are mixed types and have complex chemical composition, more versatile and universal recycling methods are required.

For other battery components, such as the graphite anodes, they are usually ignored during the recycling in most cases because of their low value. However, these materials can be used as good precursors for fabricating carbon-based functional materials, such as graphene. For this reason, the recycling of graphite anode materials should also be paid attention to in the future to produce high value-added products. Furthermore, the recycling of current collectors, electrolytes, and separator materials also requires appropriate technologies, which have been rarely investigated at the moment.

In summary, the major technologies for recycling the LiFePO_4 and $\text{LiNi}_{1-x}\text{Co}_y\text{Mn}_2\text{O}_4$ cathode materials by hydrometallurgical regeneration and direct regeneration method, and the technologies for recycling graphite anode are shown in Fig. 23.

Despite the fact that the research of recycling of the spent LNCM and LFP batteries in laboratory scale is developing rapidly, there are still many remaining challenges existing at present in industrial-scale recycling, such as the cost, safety, environment friendliness, energy consumption, efficiency, and value of the products. Considering these challenges and the above-mentioned recycling strategies, we believe that hydrometallurgical regeneration of cathode and direct regeneration are two very promising methods that could solve the issues brought by large quantities of spent LIBs of EVs and regenerate fresh cathode materials to be reused in EVs or other fields. In terms of future development of these two methods, researches should focus more on the repeatability of the regeneration process to ensure the quality consistency of the cathodes.

Declaration of Competing Interest

The authors declare that they have no known competing financial interests or personal relationships that could have appeared to influence the work reported in this paper.

Acknowledgements

This work was supported by the National Natural Science Foundation of China (Nos. 51072130, 51502045 and 21905202) and the Australian Research Council (ARC) through Discovery Early Career Researcher Award (DECRA, No. DE170100871) program.

References

- [1] R.A. Kerr, *Science* 281 (1998) 1128–1131.
- [2] N.A. Owen, O.R. Inderwildi, D.A. King, *Energy Policy* 38 (2010) 4743–4749.

- [3] A. Ullah, A. Majid, N. Rani, J. Energy Chem. 27 (2018) 219–237.
- [4] C. Yan, H. Yuan, H.S. Park, J.-Q. Huang, J. Energy Chem. 47 (2020) 217–220.
- [5] M. Zhao, B.Q. Li, H.J. Peng, H. Yuan, J.Y. Wei, J.Q. Huang, Angew. Chem. Int. Ed. (2020).
- [6] J. Xu, D. Su, W. Bao, Y. Zhao, X. Xie, G. Wang, J. Alloy. Compd. 684 (2016) 691–698.
- [7] L. Yun, D. Linh, L. Shui, X. Peng, A. Garg, M.L.P. Le, S. Asghari, J. Sandoval, Resour. Conserv. Recy. 136 (2018) 198–208.
- [8] D. Bin, Y. Wen, Y. Wang, Y. Xia, J. Energy Chem. 27 (2018) 1521–1535.
- [9] X. Shen, Z. Tian, R. Fan, L. Shao, D. Zhang, G. Cao, L. Kou, Y. Bai, J. Energy Chem. 27 (2018) 1067–1090.
- [10] B. Ma, Y. Huang, Z. Nie, X. Qiu, D. Su, G. Wang, J. Yuan, X. Xie, Z. Wu, RSC Adv. 9 (2019) 20424–20431.
- [11] Y. Liang, C.Z. Zhao, H. Yuan, Y. Chen, W. Zhang, J.Q. Huang, D. Yu, Y. Liu, M.M. Titirici, Y.L. Chueh, H. Yu, Q. Zhang, InfoMat 1 (2019) 6–32.
- [12] The State Council, Energy Conservation and New Energy Vehicle Industry Development Plan (2012–2020), http://www.nea.gov.cn/2012-07/10/c_131705726.htm, 2012 (accessed 30 March 2020).
- [13] Ministry of Industry and Information Technology, National Development and Reform Commission, Ministry of Science and Technology, Medium and long-term development plan for the automotive industry, <http://www.miit.gov.cn/n1146295/n1652858/n1652930/n3757018/c5600356/content.html>, 2017 (accessed 30 March 2020).
- [14] M.K. Tran, M.-T.F. Rodrigues, K. Kato, G. Babu, P.M. Ajayan, Nat. Energy 4 (2019) 339–345.
- [15] X. Zhang, L. Li, E. Fan, Q. Xue, Y. Bian, F. Wu, R. Chen, Chem. Soc. Rev. 47 (2018) 7239–7302.
- [16] M. Okubo, E. Hosono, J. Kim, M. Enomoto, N. Kojima, T. Kudo, H.S. Zhou, I. Honma, J. Am. Chem. Soc. 129 (2007) 7444–7452.
- [17] F. Luo, C. Wei, C. Zhang, H. Gao, J. Niu, W. Ma, Z. Peng, Y. Bai, Z. Zhang, J. Energy Chem. 44 (2020) 138–146.
- [18] L. Yang, G. Xi, Y. Xi, Ceram. Int. 41 (2015) 11498–11503.
- [19] S. Xia, W. Huang, X. Shen, J. Liu, F. Cheng, J.-J. Liu, X. Yang, H. Guo, J. Energy Chem. 45 (2020) 110–118.
- [20] K. Kretschmer, B. Sun, D. Su, Y. Zhao, G. Wang, ChemElectroChem 2 (2015) 2096–2103.
- [21] M. Li, J. Lu, Z. Chen, K. Amine, Adv. Mater. (2018) e1800561.
- [22] K. Turcheniuk, D. Bondarev, V. Singh, G. Yushin, Nature 559 (2018) 467–470.
- [23] T. Zhang, Y. He, F. Wang, H. Li, C. Duan, C. Wu, Sep. Purif. Technol. 138 (2014) 21–27.
- [24] T. Zhang, Y.Q. He, F.F. Wang, L.H. Ge, X.N. Zhu, H. Li, Waste Manage. 34 (2014) 1051–1058.
- [25] J. Wei, S. Zhao, L. Ji, T. Zhou, Y. Miao, K. Scott, D. Li, J. Yang, X. Wu, Resour. Conserv. Recy. 129 (2018) 135–142.
- [26] G. Cai, K.Y. Fung, K.M. Ng, C. Wibowo, Ind. Eng. Chem. Res. 53 (2014) 18245–18259.
- [27] Ministry of Industry and Information Technology, Ministry of Energy Conservation and Comprehensive Utilization, Research report on the recycling and utilization of the batteries retired from the electric vehicles, <http://www.miit.gov.cn/n1146285/n1146352/n3054355/n3057542/n3057547/c6651773/content.html>, 2019 (accessed 30 March 2020).
- [28] L.H. Han, Dilong; Liu Aiju; Ma Domei, Chin. J. Power Sources 38 (2014) 548–550.
- [29] B. Huang, Z. Pan, X. Su, L. An, J. Power Sources 399 (2018) 274–286.
- [30] M. Chen, X. Ma, B. Chen, R. Arsenault, P. Karlson, N. Simon, Y. Wang, Joule 3 (2019) 2622–2646.
- [31] G. Harper, R. Sommerville, E. Kendrick, L. Driscoll, P. Slater, R. Stolkin, A. Walton, P. Christensen, O. Heidrich, S. Lambert, A. Abbott, K. Ryder, L. Gaines, P. Anderson, Nature 575 (2019) 75–86.
- [32] Y. Yao, M. Zhu, Z. Zhao, B. Tong, Y. Fan, Z. Hua, ACS Sustain. Chem. Eng. 6 (2018) 13611–13627.
- [33] H. Zhou, X. Zhao, C. Yin, J. Li, Electrochim. Acta 291 (2018) 142–150.
- [34] Y. Shi, G. Chen, F. Liu, X. Yue, Z. Chen, ACS Energy Lett. 3 (2018) 1683–1692.
- [35] J. Li, L. Hu, H. Zhou, L. Wang, B. Zhai, S. Yang, P. Meng, R. Hu, J. Mater. Sci. Mater. Electron. 29 (2018) 17661–17669.
- [36] X. Song, T. Hu, C. Liang, H.L. Long, L. Zhou, W. Song, L. You, Z.S. Wu, J.W. Liu, RSC Adv. 7 (2017) 4783–4790.
- [37] T. Zhao, Y. Yao, M. Wang, R. Chen, Y. Yu, F. Wu, C. Zhang, ACS Appl. Mater. Interfaces 9 (2017) 25369–25376.
- [38] S. Natarajan, S. Rao Ede, H.C. Bajaj, S. Kundu, Colloid. Surf. A 543 (2018) 98–108.
- [39] Y. Guo, F. Li, H. Zhu, G. Li, J. Huang, W. He, Waste Manage. 51 (2016) 227–233.
- [40] X. Chen, Y. Zhu, W. Peng, Y. Li, G. Zhang, F. Zhang, X. Fan, J. Mater. Chem. A 5 (2017) 5880–5885.
- [41] H. Pan, Y. Shao, P. Yan, Y. Cheng, K.S. Han, Z. Nie, C. Wang, J. Yang, X. Li, P. Bhattacharya, K.T. Mueller, J. Liu, Nat. Energy 1 (2016) 39.
- [42] P. Meshram, B.D. Pandey, T.R. Mankhand, Hydrometallurgy 150 (2014) 192–208.
- [43] T.A. Atia, G. Elia, R. Hahn, P. Altimari, F. Pagnanelli, J. Energy Chem. 35 (2019) 220–227.
- [44] L. Chen, X.C. Tang, Y. Zhang, L.X. Li, Z.W. Zeng, Y. Zhang, Hydrometallurgy 108 (2011) 80–86.
- [45] J.M. Nan, D.M. Han, X.X. Zuo, J. Power Sources 152 (2005) 278–284.
- [46] Y.Q. Weng, S.M. Xu, G.Y. Huang, C.Y. Jiang, J. Hazard. Mater. 246 (2013) 163–172.
- [47] D. Song, X. Wang, E. Zhou, P. Hou, F. Guo, L. Zhang, J. Power Sources 232 (2013) 348–352.
- [48] L. Yao, Y. Feng, G. Xi, RSC Adv. 5 (2015) 44107–44114.
- [49] X. Zhang, Y. Xie, H. Cao, F. Nawaz, Y. Zhang, Waste Manage. 34 (2014) 1715–1724.
- [50] Y. Chen, N. Liu, F. Hu, L. Ye, Y. Xi, S. Yang, Waste Manage. 75 (2018) 469–476.
- [51] C. Hanisch, T. Loellhoeffel, J. Diekmann, K.J. Markley, W. Haselrieder, A. Kwade, J. Clean. Prod. 108 (2015) 301–311.
- [52] C.K. Lee, K.I. Rhee, J. Power Sources 109 (2002) 17–21.
- [53] L. Wang, J. Li, H. Zhou, Z. Huang, S. Tao, B. Zhai, L. Liu, L. Hu, J. Mater. Sci.-Mater. Electron. 29 (2018) 9283–9290.
- [54] Y. Yang, G. Huang, S. Xu, Y. He, X. Liu, Hydrometallurgy 165 (2016) 390–396.
- [55] R. Zheng, L. Zhao, W. Wang, Y. Liu, Q. Ma, D. Mu, R. Li, C. Dai, RSC Adv. 6 (2016) 43613–43625.
- [56] L.P. He, S.Y. Sun, X.F. Song, J.G. Yu, Waste Manage. 46 (2015) 523–528.
- [57] J.H. Li, P.X. Shi, Z.F. Wang, Y. Chen, C.C. Chang, Chemosphere 77 (2009) 1132–1136.
- [58] X. Zheng, Z. Zhu, X. Lin, Y. Zhang, Y. He, H. Cao, Z. Sun, Engineering 4 (2018) 361–370.
- [59] X. Wang, X. Wang, R. Zhang, Y. Wang, H. Shu, Waste Manage. 78 (2018) 208–216.
- [60] M. Wang, Q. Tan, L. Liu, J. Li, ACS Sustain. Chem. Eng. 7 (2019) 12799–12806.
- [61] L. Li, Y. Bian, X. Zhang, Y. Guan, E. Fan, F. Wu, R. Chen, Waste Manage. 71 (2018) 362–371.
- [62] S. Fu, X. Chen, P. Liu, W. Liu, P. Liu, K. Zhang, H. Chen, J. Mater. Eng. Perform. 27 (2018) 5511–5517.
- [63] L. Li, E. Fan, Y. Guan, X. Zhang, Q. Xue, L. Wei, F. Wu, R. Chen, ACS Sustain. Chem. Eng. 5 (2017) 5224–5233.
- [64] Q. Meng, Y. Zhang, P. Dong, F. Liang, J. Ind. Eng. Chem. 61 (2018) 133–141.
- [65] H. Ebrahizadeh, G.R. Khayati, M. Schaffie, J. Mater. Cycles Waste 20 (2018) 2117–2129.
- [66] W. Gao, J. Song, H. Cao, X. Lin, X. Zhang, X. Zheng, Y. Zhang, Z. Sun, J. Clean. Prod. 178 (2018) 833–845.
- [67] L.-P. He, S.-Y. Sun, Y.-Y. Mu, X.-F. Song, J.-G. Yu, ACS Sustain. Chem. Eng. 5 (2016) 714–721.
- [68] C. Sun, L. Xu, X. Chen, T. Qiu, T. Zhou, Waste Manage. Res. 36 (2018) 113–120.
- [69] L. Zhuang, C. Sun, T. Zhou, H. Li, A. Dai, Waste Manage. 85 (2019) 175–185.
- [70] R. Sattar, S. Ilyas, H.N. Bhatti, A. Ghaffar, Sep. Purif. Technol. 209 (2019) 725–733.
- [71] W.-S. Chen, H.-J. Ho, Metals 8 (2018) 321.
- [72] N. Vieceli, C.A. Nogueira, C. Guimaraes, M.F.C. Pereira, F.O. Durao, F. Margarido, Waste Manage. 71 (2018) 350–361.
- [73] W. Lv, Z. Wang, H. Cao, X. Zheng, W. Jin, Y. Zhang, Z. Sun, Waste Manage. 79 (2018) 545–553.
- [74] F. Pagnanelli, E. Moscardini, P. Altimari, T.A. Atia, L. Toro, Waste Manage. 60 (2017) 706–715.
- [75] P. Liu, L. Xiao, Y. Chen, Y. Tang, J. Wu, H. Chen, J. Alloy. Compd. 783 (2019) 743–752.
- [76] J. Hu, J. Zhang, H. Li, Y. Chen, C. Wang, J. Power Sources 351 (2017) 192–199.
- [77] Y. Huang, G. Han, J. Liu, W. Chai, W. Wang, S. Yang, S. Su, J. Power Sources 325 (2016) 555–564.
- [78] E.J. Shin, S. Kim, J.-K. Noh, D. Byun, K.Y. Chung, H.-S. Kim, B.-W. Cho, J. Mater. Chem. A 3 (2015) 11493–11502.
- [79] H. Li, S. Xing, Y. Liu, F. Li, H. Guo, G. Kuang, ACS Sustain. Chem. Eng. 5 (2017) 8017–8024.
- [80] D. Bian, Y. Sun, S. Li, Y. Tian, Z. Yang, X. Fan, W. Zhang, Electrochim. Acta 190 (2016) 134–140.
- [81] J. Zhang, J. Hu, Y. Liu, Q. Jing, C. Yang, Y. Chen, C. Wang, ACS Sustain. Chem. Eng. (2019) 5626–5631.
- [82] W.-Y. Wang, C.H. Yen, J.-L. Lin, R.-B. Xu, J. Mater. Cycles Waste 21 (2019) 300–307.
- [83] J. Zhang, J. Hu, W. Zhang, Y. Chen, C. Wang, J. Clean. Prod. 204 (2018) 437–446.
- [84] E. Billy, M. Joulie, R. Laucournet, A. Boulineau, E. De Vito, D. Meyer, ACS Appl. Mater. Interfaces 10 (2018) 16424–16435.
- [85] A.A. Nayil, R.A. Elkhashab, S.M. Badawy, M.A. El-Khateeb, Arab. J. Chem. 10 (2017) S3632–S3639.
- [86] L.-P. He, S.-Y. Sun, X.-F. Song, J.-G. Yu, Waste Manage. 64 (2017) 171–181.
- [87] P. Meshram, B.D. Pandey, T.R. Mankhand, Waste Manage. 45 (2015) 306–313.
- [88] P. Meshram, B.D. Pandey, T.R. Mankhand, Chem. Eng. J. 281 (2015) 418–427.
- [89] Y. Yang, X. Zheng, H. Cao, C. Zhao, X. Lin, P. Ning, Y. Zhang, W. Jin, Z. Sun, ACS Sustain. Chem. Eng. 5 (2017) 9972–9980.
- [90] L. Li, J. Ge, F. Wu, R. Chen, S. Chen, B. Wu, J. Hazard. Mater. 176 (2010) 288–293.
- [91] R. Golmohammadzadeh, F. Faraji, F. Rashchi, Resour. Conserv. Recy. 136 (2018) 418–435.
- [92] L. Li, Y. Bian, X. Zhang, Q. Xue, E. Fan, F. Wu, R. Chen, J. Power Sources 377 (2018) 70–79.
- [93] L. Sun, K. Qiu, Waste Manage. 32 (2012) 1575–1582.
- [94] X. Zhang, Y. Bian, S. Xu, E. Fan, Q. Xue, Y. Guan, F. Wu, L. Li, R. Chen, ACS Sustain. Chem. Eng. 6 (2018) 5959–5968.
- [95] L.-P. He, S.-Y. Sun, J.-G. Yu, Ceram. Int. 44 (2018) 351–357.
- [96] X. Chen, B. Fan, L. Xu, T. Zhou, J. Kong, J. Clean. Prod. 112 (2016) 3562–3570.
- [97] D. Pant, T. Dolker, Waste Manage. 60 (2017) 689–695.
- [98] W. Gao, X. Zhang, X. Zheng, X. Lin, H. Cao, Y. Zhi, Z. Sun, Environ. Sci. Technol. 51 (2017) 1662–1669.
- [99] L. Yao, H. Yao, G. Xi, Y. Feng, RSC Adv. 6 (2016) 17947–17954.

- [100] J. Ren, Y. Zhang, W. Bai, X. Chen, Z. Zhang, X. Fang, W. Weng, Y. Wang, H. Peng, *Angew. Chem. Int. Ed. Engl.* 53 (2014) 7864–7869.
- [101] X. Zhang, H. Cao, Y. Xie, P. Ning, H. An, H. You, F. Nawaz, *Sep. Purif. Technol.* 150 (2015) 186–195.
- [102] E. Fan, L. Li, X. Zhang, Y. Bian, Q. Xue, J. Wu, F. Wu, R. Chen, *ACS Sustain. Chem. Eng.* 6 (2018) 11029–11035.
- [103] H. Ku, Y. Jung, M. Jo, S. Park, S. Kim, D. Yang, K. Rhee, E.-M. An, J. Sohn, K. Kwon, *J. Hazard. Mater.* 313 (2016) 138–146.
- [104] X. Zheng, W. Gao, X. Zhang, M. He, X. Lin, H. Cao, Y. Zhang, Z. Sun, *Waste Manage.* 60 (2017) 680–688.
- [105] H. Wang, K. Huang, Y. Zhang, X. Chen, W. Jin, S. Zheng, Y. Zhang, P. Li, *ACS Sustain. Chem. Eng.* 5 (2017) 11489–11495.
- [106] X. Meng, K.N. Han, *Miner. Process. Extr. Metall. Rev.* 16 (1996) 23–61.
- [107] M. Zuniga, F. Parada, L.E. Asselin, *Hydrometallurgy* 104 (2010) 260–267.
- [108] A. van Bommel, J.R. Dahn, *Chem. Mater.* 21 (2009) 1500–1503.
- [109] P. Liu, L. Xiao, Y. Tang, Y. Zhu, H. Chen, Y. Chen, *Vacuum* 156 (2018) 317–324.
- [110] B.P. Xin, D. Zhang, X. Zhang, Y.T. Xia, F. Wu, S. Chen, L. Li, *Bioresour. Technol.* 100 (2009) 6163–6169.
- [111] Z.R. Niu, Y.K. Zou, B.P. Xin, S. Chen, C.H. Liu, Y.P. Li, *Chemosphere* 109 (2014) 92–98.
- [112] Y. Xin, X. Guo, S. Chen, J. Wang, F. Wu, B. Xin, *J. Clean. Prod.* 116 (2016) 249–258.
- [113] D. Santhiya, Y.P. Ting, *J. Biotechnol.* 116 (2005) 171–184.
- [114] N. Bahaloo-Horeh, S.M. Mousavi, *Waste Manage.* 60 (2017) 666–679.
- [115] N. Bahaloo-Horeh, S.M. Mousavi, M. Baniasadi, *J. Clean. Prod.* 197 (2018) 1546–1557.
- [116] C.H. Lee, M.K. Jeong, M.F. Kilicaslan, J.H. Lee, H.S. Hong, S.J. Hong, *Waste Manage.* 33 (2013) 730–734.
- [117] W.Y. Yuan, J.H. Li, Q.Q. Zhang, F. Saito, B. Yang, *J. Air Waste Manage. Assoc.* 63 (2013) 418–423.
- [118] C.F. Burmeister, A. Kwade, *Chem. Soc. Rev.* 42 (2013) 7660–7667.
- [119] Q. Tan, J. Li, *Environ. Sci. Technol.* 49 (2015) 5849–5861.
- [120] Y. Liu, X. Chi, Q. Han, Y. Du, J. Huang, Y. Liu, J. Yang, *J. Power Sources* 443 (2019).
- [121] M.M. Wang, C.C. Zhang, F.S. Zhang, *Waste Manage.* 51 (2016) 239–244.
- [122] M.M. Wang, C.C. Zhang, F.S. Zhang, *Waste Manage.* 67 (2017) 232–239.
- [123] J. Sencanski, D. Bajuk-Bogdanovic, D. Majstorovic, E. Tchernychova, J. Papan, M. Vujkovic, *J. Power Sources* 342 (2017) 690–703.
- [124] Z. Zheng, M. Chen, Q. Wang, Y. Zhang, X. Ma, C. Shen, D. Xu, J. Liu, Y. Liu, P. Gonet, I. O'Connor, L. Pinnell, J. Wang, E. Gratz, R. Arsenault, Y. Wang, *ACS Sustain. Chem. Eng.* 6 (2018) 13977–13982.
- [125] S.H. Park, S.H. Kang, I. Belharouak, Y.K. Sun, K. Amine, *J. Power Sources* 177 (2008) 177–183.
- [126] M. Song, H. Tan, D. Chao, H.J. Fan, *Adv. Funct. Mater.* 28 (2018) 1802564.
- [127] X. Chen, C. Guo, H. Ma, J. Li, T. Zhou, L. Cao, D. Kang, *Waste Manage.* 75 (2018) 459–468.
- [128] R. Zheng, W. Wang, Y. Dai, Q. Ma, Y. Liu, D. Mu, R. Li, J. Ren, C. Dai, *Green. Energy Environ.* 2 (2017) 42–50.
- [129] Y. Liu, M. Liu, *Int. J. Hydrog. Energy* 42 (2017) 18189–18195.
- [130] Y. Yang, G. Huang, M. Xie, S. Xu, Y. He, *Hydrometallurgy* 165 (2016) 358–369.
- [131] Q. Sa, E. Gratz, J.A. Heelan, S. Ma, D. Apelian, Y. Wang, *J. Sustain. Metall.* 2 (2016) 248–256.
- [132] Q. Sa, E. Gratz, M. He, W. Lu, D. Apelian, Y. Wang, *J. Power Sources* 282 (2015) 140–145.
- [133] L. Li, X. Zhang, R. Chen, T. Zhao, J. Lu, F. Wu, K. Amine, *J. Power Sources* 249 (2014) 28–34.
- [134] E. Gratz, Q. Sa, D. Apelian, Y. Wang, *J. Power Sources* 262 (2014) 255–262.
- [135] H. Zou, E. Gratz, D. Apelian, Y. Wang, *Green Chem.* 15 (2013) 1183–1191.
- [136] J. Chen, Q. Li, J. Song, D. Song, L. Zhang, X. Shi, *Green Chem.* 18 (2016) 2500–2506.
- [137] X. Zhang, Q. Xue, L. Li, E. Fan, F. Wu, R. Chen, *ACS Sustain. Chem. Eng.* 4 (2016) 7041–7049.
- [138] X. Li, J. Zhang, D. Song, J. Song, L. Zhang, *J. Power Sources* 345 (2017) 78–84.
- [139] W. Song, J. Liu, L. You, S. Wang, Q. Zhou, Y. Gao, R. Yin, W. Xu, Z. Guo, *J. Power Sources* 419 (2019) 192–202.
- [140] X. Meng, J. Hao, H. Cao, X. Lin, P. Ning, X. Zheng, J. Chang, X. Zhang, B. Wang, Z. Sun, *Waste Manage.* 84 (2019) 54–63.
- [141] B. Xu, P. Dong, J. Duan, D. Wang, X. Huang, Y. Zhang, *Ceram. Int.* 45 (2019) (1801) 11792–11800.
- [142] Nat. Energy 4 (2019) 253–253.
- [143] B. Moradi, G.G. Botte, *J. Appl. Electrochem.* 46 (2015) 123–148.
- [144] H.S. Hou, X.Q. Qiu, W.F. Wei, Y. Zhang, X.B. Ji, *Adv. Energy Mater.* 7 (2017) 1602898.
- [145] Z. Ma, Y. Zhuang, Y. Deng, X. Song, X. Zuo, X. Xiao, J. Nan, *J. Power Sources* 376 (2018) 91–99.
- [146] Y. Yang, S. Song, S. Lei, W. Sun, H. Hou, F. Jiang, X. Ji, W. Zhao, Y. Hu, *Waste Manage.* 85 (2019) 529–537.
- [147] Z. Cao, X. Zheng, H. Cao, H. Zhao, Z. Sun, Z. Guo, K. Wang, B. Zhou, *Chem. Eng. J.* 337 (2018) 256–264.
- [148] S. Natarajan, D. Shanthana Lakshmi, H.C. Bajaj, D.N. Srivastava, *J. Environ. Chem. Eng.* 3 (2015) 2538–2545.
- [149] K.S. Novoselov, A.K. Geim, S.V. Morozov, D. Jiang, Y. Zhang, S.V. Dubonos, I.V. Grigorieva, A.A. Firsov, *Science* 306 (2004) 666–669.
- [150] A.K. Geim, K.S. Novoselov, *Nat. Mater.* 6 (2007) 183–191.
- [151] K.S. Novoselov, V.I. Fal'ko, L. Colombo, P.R. Gellert, M.G. Schwab, K. Kim, *Nature* 490 (2012) 192–200.
- [152] Y. Zhang, N. Song, J. He, R. Chen, X. Li, *Nano Lett.* 19 (2018) 512–519.
- [153] W. Zhang, Z. Liu, J. Xia, F. Li, W. He, G. Li, J. Huang, *Front. Environ. Sci. Eng.* 11 (2017) 6.
- [154] S. Natarajan, H.C. Bajaj, V. Aravindan, *J. Mater. Chem. A* 7 (2019) 3244–3252.
- [155] K. Meng, Y. Cao, B. Zhang, X. Ou, D.-M. Li, J.-F. Zhang, X. Ji, *ACS Sustain. Chem. Eng.* 7 (2019) 7750–7759.
- [156] F. Wu, J. Tian, Y. Su, J. Wang, C. Zhang, L. Bao, T. He, J. Li, S. Chen, *ACS Appl. Mater. Interfaces* 7 (2015) 7702–7708.
- [157] X. Xiong, Z. Wang, H. Guo, Q. Zhang, X. Li, *J. Mater. Chem. A* 1 (2013) 1284–1288.
- [158] K. Min, S.-W. Seo, Y.Y. Song, H.S. Lee, E. Cho, *Phys. Chem. Chem. Phys.* 19 (2017) 1762–1769.
- [159] Y. Zou, X. Yang, C. Lv, T. Liu, Y. Xia, L. Shang, G.I. Waterhouse, D. Yang, T. Zhang, *Adv. Sci. (Weinh)* 4 (2017) 1600262.
- [160] J. Li, Y. Wang, L. Wang, B. Liu, H. Zhou, *J. Mater. Sci.-Mater. Electron.* 30 (2019) 14580–14588.
- [161] E. Shangguan, Q. Wang, C. Wu, S. Wu, M. Ji, J. Li, Z. Chang, Q. Li, *ACS Sustain. Chem. Eng.* 6 (2018) 13312–13323.
- [162] E. Shangguan, S. Fu, S. Wu, Q. Wang, C. Wu, J. Li, X. Cai, Z. Chang, Z. Wang, Q. Li, K. Jiang, *J. Power Sources* 403 (2018) 38–48.
- [163] S. Natarajan, V. Aravindan, *ACS Energy Lett.* 3 (2018) 2101–2103.